NASA Technical Memorandum 81926

NASA-TM-81926 19810007619

MECHANISMS OF FATIGUE DAMAGE IN BORON/ALUMINUM COMPOSITES

W. S. Johnson

DECEMBER 1980

NASA
National Aeronautics and Space Administration

Langley Research Center
Hampton, Virginia 23665

MECHANISMS OF FATIGUE DAMAGE IN BORON/ALUMINUM COMPOSITES

W. S. Johnson
NASA Langley Research Center
Hampton, Virginia 23665

ABSTRACT

Fatigue damage mechanisms have been investigated using a series of tensile fatigue tests on several laminates of boron/aluminum (6061-0). This study focused on four aspects of the fatigue response. First, in laminates with 0° fibers on the outside, an analysis that identifies "shakedown" conditions was shown to predict the stress amplitude below which no fatigue damage accumulated. Second, a simple fatigue damage accumulation model which relates matrix fatigue cracking and the overall laminate properties is described. A model for the saturation damage stage development is presented. Third, data will illustrate that identical laminates, tested in directions 90° apart (such that one layup has 90° outer plies and the other 0°), have different fatigue behaviors due to the stacking sequence. The 90° plies on the surface develop cracks earlier than predicted by shakedown. An attempt was made to explain this stacking sequence effect. Finally, variable load history effects on the fatigue damage response were investigated by simple tests. These tests revealed that for a given stress ratio the specimen seeks the saturation damage state for the largest stress range to which it is subjected. It was also found that little damage is generated by shifting a given stress range down, whereas significant damage may be created by shifting it upward. The laminate stresses were always tensile.

LIST OF SYMBOLS

a	half length of crack, mm
E^f	fiber elastic modulus, MPa
E^m	matrix elastic modulus, MPa
E^m_{eff}	effective modulus of the matrix in the loading direction, MPa
E_N	unloading elastic modulus of the Nth cycle, MPa
E_o	unloading elastic modulus of the first cycle, MPa
R	stress ratio
S_{max}	maximum laminate stress, MPa
S_{min}	minimum laminate stress, MPa
S_{11}	laminate stress in the 0^o fiber direction, MPa
S_{22}	laminate stress in the 90^o fiber direction, MPa
S_{33}	laminate stress in the thickness direction, MPa
V_f	fiber volume fraction
Y	cyclic hardened yield stress, corresponds to one-half the matrix fatigue limit for $R = 0$, MPa
$\Delta\varepsilon$	laminate strain range associated with the saturation damage state
$\Delta\varepsilon^m_{comp}$	compressive strain range of the matrix material in the loading direction
ΔK	stress intensity range, $MN\text{-}m^{-3/2}$
ΔK_{th}	threshold stress intensity range, $MN\text{-}m^{-3/2}$
ΔS	laminate stress range, MPa

ΔS_{sh} stress range that causes no fatigue damage, MPa

$\Delta\sigma_e$ stress required to growth an embedded flaw, MPa

$\Delta\sigma_s$ stress required to grow a surface flaw, MPa

ν^f Poisson's ratio of the boron fiber

ν^m Poisson's ratio of the matrix material

ϕ correction factor to account for the effect of laminate stacking sequence

INTRODUCTION

In recent years, fatigue damage and failure of metal-matrix fibrous composites have been extensively studied [1-11]. Most studies were tests to determine S-N curves. Such tests indicate only the number of cycles that a composite laminate could sustain for constant maximum and minimum load levels; they do not indicate the physical degradation due to fatigue, nor give much insight into the complex fatigue damage mechanisms that occur in these materials. Most fatigue tests of metal matrix composites were conducted under constant amplitude loading; thus, variable amplitude loading effects, which are prominent in most structural applications, are not well understood.

The objective of this paper is to examine, by test, the fatigue damage mechanisms of continuous boron fibers in a 6061 aluminum matrix. It will focus on four areas of metal matrix fatigue: (1) correlation of laminate fatigue damage threshold with the matrix cyclic yield stress, (2) presentation of a simple model for the damage

that leads to a damage saturation state, (3) the effect of ply stacking sequence on fatigue damage accumulation, and (4) the effect of variable load history on fatigue damage.

FATIGUE OF COMPOSITE LAMINATES

Specimen Preparation and Testing

The material for the boron-aluminum composite specimens was manufactured in the form of 300 by 230 mm plates. The matrix was 6061 aluminum; fibers were 0.14 mm (5.6 mils) diameter boron.

Table 1 presents material properties for the boron 28 and aluminum constituents and Table 2 shows the six laminates that were tested. Plates were cut with a diamond saw into rectangular specimens 102 mm (4.0 in.) long and 12.7 mm (0.50 in.) wide. All specimens were annealed at 413° C (775° F) for two hours and cooled at the rate of about 28° C (50° F) per hour from the annealing temperature to 260° C (500° F), oven cooled to room temperature. Ultrasonic C-scan was used to screen out the specimens containing detectable defects (see Appendix). Glass-epoxy end tabs were bonded to each composite specimen. Tab dimensions were 3.2 mm (0.125 in.) thick and 28.6 mm (1.125 in.) long. All fatigue failures occurred in the gage section, none in the tab area.

The specimens were tested at a cyclic frequency of 10 Hz in an MTS closed-loop hydraulic machine, in a load-controlled tension-tension mode. Standard wedge grips were used. The specimen

strains were measured with an MTS extensometer of 25.4 mm (1.0 in.) gage length, designed for fatigue testing. An X-Y plotter recorded the stress-strain response during a quasi-static loading cycle.

Boron-Aluminum Composite Test Results

As previously mentioned, the stress-strain response of each specimen was recorded at various intervals during the cyclic life to determine the changes in various mechanical properties due to fatigue damage. These changes in mechaincal properties will be shown to be caused primarily by fatigue cracks developing in the matrix material. Figure 1 shows a typical stress-strain response of a boron-aluminum laminate loaded at $R = 0.3$. The unloading elastic modulus was measured for each recorded cycle. Secant modulus is affected by matrix hardening as well as fatigue damage [12,13] whereas the unloading elastic modulus is not, and is a more direct indicator of fatigue damage.

An example of the fatigue damage accumulation as a function of number of applied cycles and stress is presented in Figure 2 for a $[0/\pm 45/90/0/\pm 45/\overline{90}]_s$ laminate. The damage is expressed in terms of E_N/E_o, the percent of the initial unloading elastic modulus remaining after N cycles. All of the data shown are for specimens that survived 2-million cycles, after which the tests were terminated. Notice that each specimen appears to reach a stabilized

value of E_N/E_o herein referred to as a "saturation damage state" (SDS). All of the specimens shown in Figure 2 were cyclic loaded below the 375 MPa fatigue limit. S-N data and the associated fatigue limits are presented in reference [13] for all six laminates. The saturation damage state implies that the laminate will neither accumulate more damage or fail under the present loading condition.

Figure 3 presents the saturation damage state as a function of stress range by plotting the E_N/E_o values after two million cycles. This figure includes data for stress ratios of $R = 0.1$ and 0.3. The constant amplitude saturation damage state sums to be a function of stress range and independent of mean stress. The data can be extrapolated, using a regression analysis, to 100 percent of E_N/E_o (i.e., no change in elastic unloading modulus) to determine the stress range below which no fatigue damage accumulates. This range was referred to as the shakedown range ΔS_{sh}. The type of data presented above was generated for all six laminates. The corresponding ΔS_{sh} values are presented in Table 2. Notice that the laminates with a 90^o ply on the surface have lower ΔS_{sh} values than similar laminates with 0^o surface plies. Hence, the stress level required to produce fatigue damage is lower for laminates with 90^o outer plies than for those with 0^o outer plies. This stacking sequence effect will be discussed later.

Shakedown Analysis

The possible relationship between fatigue and shakedown stress range in metal matrix composites was first suggested by

Dvorak and Tarn [14] and related to the available experimental data, obtained primarily for unidirectional B-Aℓ materials. Since only S-N data were available for analysis, they tried to relate the shakedown stress to the fatigue limit. This relationship, however, does not generally hold, as was demonstrated when additional data became available. In the present paper, the relationship between the fatigue damage initiation stress (not fatigue limit) and shakedown is examined analytically and experimentally for both unidirectional and cross-plied B-Aℓ composites.

If fatigue damage is to be avoided in general, and low cycle fatigue failures in particular, the cyclic applied load must produce only elastic strains in all constituents. However, local plastic straining can be permitted in the composite during the first few load cycles, provided that the composite "shakes down" during these few cycles. The shakedown state is reached if the matrix cyclically hardens to a cyclic yield stress Y such that only elastic deformation occurs under the subsequent load cycles. Previous tests on annealed aluminum have shown that the fatigue limit coincides with the stable cyclic yield stress [15], i.e. the cyclic range was elastic. This is in accordance with Melan's theorem [16] as well as others [17-19].

The application of Melan's theorem to shakedown of unidirectional composites was presented in [20] and the extension to laminate plates

was discussed in [12]. These and other related results [21-23] describe a procedure for the determination of initial yield surfaces for composite laminates, the translation of these surfaces in the load space during plastic loading, and their relation to shakedown envelopes.

Figure 4 shows the ply yield surfaces for the case of a B-Aℓ plate under biaxial in-plane stresses S_{11} and S_{22}; Y is the cyclic hardened yield strength of the aluminum matrix. Each of the plies has its own elliptical yield surface, constructed analytically from the ply matrix stresses and the Mises yield condition. The overall yield surface of the laminate is an internal envelope of the yield surfaces of individual plies.

Figure 5 shows this internal envelope, i.e., the laminate initial yield surface, and the translation and deformation of this yield surface in the process of plastic loading to $S_{11}/Y = 3.0$. The deformation of the laminate yield surface is the result of the relative translation of the three ply yield surfaces in the biaxial loading plane. Each of the ply surfaces translates, according to its own hardening rule [22-24]. After loading to $S_{11}/Y = 3.0$, the composite will remain elastic for any loading path within the current yield surface. In the case of cyclic loading, the current yield surface will be the shakedown envelope, such as the envelope shown in Figure 5. The shakedown stress range, ΔS_{sh}, is the

width of the shakedown envelope in the direction of uniaxial loading applied in this experimental program.

$\Delta S_{sh}/Y$ is the dimensionless width of the internal envelope of the yield surfaces along the S_{11} load axis in Figures 4 and 5. The analytically predicted magnitudes of $\Delta S_{sh}/Y$ are listed in Table 2. In each case load applied is applied in the 0^{o} fiber direction.

Unreinforced 6061-0 aluminum specimens were fatigue tested to determine the extent of cyclic hardening and the appropriate value for Y that may be expected for the matrix of the composite specimens. The average initial yield stress of six specimens was found to be 58.0 MPa (8.42 ksi). The maximum elastic stress range corresponded to the fatigue limit, which was 141 MPa (20.4 ksi) at 2×10^{6} cycles. The magnitude of matrix yield stress Y to be used in shakedown limit calculations was assumed to be 70.3 MPa (10.2 ksi), i.e., to one-half of the fatigue limit at $R \approx 0.1$. This R value is not quite ideal because the matrix, within a composite containing 0^{o} fibers, cycles between its tensile and compressive yield stress, Y, at $R = -1.0$. More details are available in references [12] and [13].

Table 2 presents the analytical shakedown range and the range determined from the regression analysis of the experimental data. The correlation is within 10 percent except for those laminates

with 90° outer plies. This suggests that there exists a stacking sequence effect.

SIMPLE FATIGUE DAMAGE MODEL

The decrease in elastic unloading modulus observed during fatigue cycling could be caused by matrix cracking or fiber breakage. Specimens were examined for fiber failure and matrix cracking by gradual etching of the aluminum matrix in a 30 percent HCℓ solution in distilled water. Fiber failure was detected only in specimens tested at stresses that approached the fatigue limit. However, substantial laminate modulus changes were detected well below this stress level. Those specimens that sustained modulus loss without failure had long matrix cracks which grew parallel to the fibers in the off-axis layers of the laminate. These cracks appeared to be mostly within the individual off-axis plies. They did not extend beyond the nearest layer of fibers that were not parallel to the matrix crack direction. Almost all of the observed modulus decrease is likely to be attributable to cracks in the off-axis plies, since such cracks were the only observed damage of consequence.

Figure 6 shows the matrix cracks in the 45° layer of a $[0/\pm45/90/0/\pm45/\overline{90}]_s$ specimen tested at S_{max} = 375 MPa, R = 0.3, for 2×10^6 cycles. The cracks are partially hidden behind the few remaining 0° (vertical) fibers (oriented in the vertical direction in Figure 6). No matrix cracks were seen on the outer surface,

other than an occasional "H" crack [9,12] associated with a random broken 0° fiber.

Figure 7 reveals the matrix cracking in the second ply of a $[0/90]_{2s}$ laminate specimen tested at S_{max} = 500 MPa, R = 0.1 for 2 x 10^6 cycles.

A simple analysis was developed to relate the decrease in laminate unloading elastic modulus to the matrix damage. The off-axis plies were assumed to develop cracks during cyclic loading (above the shakedown stress range) so that the cracks opened during tensile loading; thus, the modulus is reduced under tensile loads in the matrix. However, for compressive loading the cracks close, so the modulus is unchanged. Figure 8 illustrates this behavior in terms of the applied laminate stress and the corresponding stresses in the matrix and 0° fibers. The laminate has an ideally elastic-plastic matrix (for illustration of the model and simplicity of presentation) and is subjected to a constant cyclic stress range, ΔS. The matrix stress was assumed to cycle between +Y and -Y as shown in Figure 8. The dashed lines in this figure represent the initial loading response. Accordingly, the first load cycle causes the matrix and 0°-fiber stresses to follow the dashed loops. With subsequent cycling, the matrix cracks, effectively decrease the matrix tensile modulus until a saturation damage state is reached. The dashed loops narrow to zero-width loops, shown as solid lines; the lines represent the

saturation damage state. The saturation damage state develops when the matrix cracking causes transfers of load to the 0° fibers, thus relieving the matrix from undergoing additional damaging plastic deformation. If the stress range, ΔS, were increased, the effective tensile modulus of the matrix must decrease to again reach a saturation damage state, which implies that more fatigue damage must occur. The laminate elastic unloading modulus would then decrease even more. If the load transferred to the 0° fiber due to matrix cracking and overall laminate load, causes the 0° fiber stress to exceed the fiber's endurance strength, σ^{f}_{ult}, no saturation damage state will develop; the laminate will fail.

The drop in matrix modulus in the load direction due to fatigue damage will now be evaluated. Figure 9 depicts the stress-strain curve of the saturation damage state that has developed a hypothetical laminate. The strain in the matrix and laminate is plotted versus the matrix stress, σ^{m}, and laminate stress, S, respectively. The damage state has an associated cyclic strain range, $\Delta\varepsilon$, that remains constant during a saturation damage state [13]. If this cyclic strain range is known, an effective tensile modulus E^{m}_{eff} of the off-axis matrix material can be estimated. Note that E^{m}_{eff} is the modulus in the loading (0°-fiber) direction. The compressive strain range of the matrix, $\Delta\varepsilon^{m}_{comp}$, was approximated by

$$\Delta\varepsilon^{m}_{comp} = \frac{\Delta S_{sh}}{2E_{o}}$$

where S_{sh} and E_o are the experimentally determined shakedown stress range and initial laminate unloading elastic modulus, respectively. The effective tensile modulus of the off-axis matrix material can now be approximated by dividing Y by the cyclic strain minus the compressive portion,

$$E^m_{eff} = Y \Big/ \left(\Delta\varepsilon - \frac{\Delta S_{sh}}{2E_o} \right)$$

where $Y = 70.3$ MPa for laminates with 0° outer laminae, which correlated well with the shakedown analysis; however,

$$E^m_{eff} = Y\phi \Big/ \left(\Delta\varepsilon - \frac{\Delta S_{sh}}{2E_o} \right)$$

For the laminates with off-axis laminae on the outside the factor ϕ is introduced to correct for the effects of stacking sequence on the shakedown stress range, and is defined as

$$\phi = \frac{\Delta S_R}{\Delta S_{sh}}$$

Notice that the values of ϕ in table 2 are near unity for laminates with 0° fibers on the surface, but are much smaller for laminates with off-axis laminae on the outside. The validity of the above assumptions and model can be evaluated for other arbitrary laminates that have developed a saturation damage state by measuring the cyclic strains. The E^m_{eff} values can be calculated from the data in tables 2 and 3 and the above equations.

The E^m_{eff} were used as the matrix modulus in lamination theory (using the computer program ANSPLY [24]) to calculate the unloading elastic modulus of the composite in its saturation damage state. All the fibers were assumed to be intact, and matrix damage was assumed to be characterized by its lower modulus, E^m_{eff}. Although such a formulation implicitly assumes that the matrix modulus is reduced isotropically, the reduction really is orthotropic. However, since we are interested in the laminate modulus in the loading direction only, the assumption should not introduce excessive error. Table 3 presents the results obtained at two cyclic stress levels for each laminate. The predicted and experimental E_N/E_o values are presented for comparison. The good correlation between these experimental and predicted values lends validity to the model illustrated by figures 8 and 9. Therefore, if the cyclic strain range is known for a particular metal matrix composite laminate, a good quantitative approximation of the matrix fatigue damage in terms of elastic modulus reduction can be calculated.

It is further suggested that a saturation damage state can only be maintained within laminate specimens that contain 0^o or near 0^o laminae. The 0^o laminae enable the matrix to reach a damage state such that the matrix stresses, σ^m, are low enough that damage no longer accumulates. In other words, it is expected that an angle-ply laminate specimen, such as $(\pm 45)_s$, would fail at approximately the

laminate shakedown stress range since, once the fatigue damage starts, it could only end in failure of the laminate. Menke and Toth [7] present S-N data for $\pm 45^{\circ}$ cross-ply B-Aℓ 6061 specimens, with $V_f = 0.60$. The fatigue limit, at 2×10^6 cycles and $R = 0.0$, was 138 MPa (20 ksi). The S-N curve was very flat. The initial yield surface of this laminate was calculated, as discussed earlier in this paper, and resulted in a shakedown range of 2.14 Y. Assuming the Y for Menke and Toth's matrix is equal to the matrix material tested in this program, the shakedown range for a ± 45 laminate with $V_f = 0.6$ is $\Delta S_{sh} = 150$ MPa, which agrees well with the experimental data (i.e., 138 MPa). Therefore, the angle-ply laminate specimens probably do not reach a saturation damage state, but fail at approximately the laminate shakedown stress range due to matrix cracking.

STACKING SEQUENCE EFFECT

As shown earlier, laminates with 90° outer plies tends to accumulate fatigue damage at a lower stress level than a similar laminate with 0° outer plies (table 3). An examination of the behavior of $[0/90]_{2s}$ and $[90/0]_{2s}$ laminate specimens cut from the same plate will now illustrate this.

Figure 10 presents curves depicting modulus loss, due to 2×10^6 cycles of fatigue, versus the cyclic stress range for both $[0/90]_{2s}$ and $[90/0]_{2s}$. Notice that the $[90/0]_{2s}$ accumulates damage

at a lower fatigue stress range. However at the high stress, i.e., 400 MPa, the damage is nearly equal for both laminates.

Further evidence of the stacking sequence effect is found in a series of micrographs of $[90/0]_{2s}$ specimens (figure 11). The micrographs are of the failure surface with the 90° fibers in the plane of the page. Each specimen presented was tested at a different stress level for 2×10^{6} fatigue cycles and then pulled for residual strength. Notice in Figure 11(a) (ΔS = 202.5 MPa) that the 90° fibers are split longitudinally in all of the 90° plies. The 90° fibers split through the tungstun core, which is sometimes visible as a line in the middle of the fiber. This is an indication of very little fatigue damage in the matrix before the residual strength test. The transverse strength of the boron fiber appears to be less than undamaged matrix material. Merke and Toth [7] have made similar observations. The specimen shown in figure 11(b) (ΔS = 225 MPa), indicates cracks in the outer 90° plies, since the inner 90° still failed through the fibers, whereas the outerplies failed through the weaker cracked matrix. These cracks in the outer 90° plies were also visible on the surface. (Notice in figure 10 that at stress range equal 225 MPa the $[90/0]_{2s}$ laminate had lost 18 percent of the initial modulus, whereas the $[0/90]_{2s}$ only lost 5 percent. When examined, the $[0/90]_{2s}$ specimen revealed no significant surface damage, fiber damage, or cracks in internal ply matrices.) Figure 11(c) (ΔS = 405 MPa) shows extensive matrix damage in all four 90° plies. A $[0/90]_{2s}$ specimen tested at the same stress level also showed as much damage.

Hancock [5] stated that the fatigue damage in a composite laminate could initiate from surface imperfections. However, as previously discussed, the microscopic examinations showed that the only surface cracking found on the 0° outer layer were the H-cracks that were associated with broken 0° fibers. The microscopic examination further revealed that the 0° lamina had a crack arresting capacity for cracks growing other than parallel to the fibers. Long matrix cracks in the $+45^{\circ}$ and 90° lamina (Figures 6 and 7) grew to the edge of the 0° fibers without causing 0° fiber failure or growing past the 0° fibers to the free surface. Therefore, if potential crack initiation sites existed on the free surface, it is doubtful that they could initiate and grow because of the restraint of the 0° fibers.

However, with the 90° fibers on the free surface, the surface defects could indeed cause early crack initiation and growth. Figure 11(b) illustrated the crack growth in the outer 90° surface as opposed to little or no cracking in the inner two 90° plies. This can be explained by the use of fracture mechanics. Assume that there exists two tiny flaws of the same dimension $\underline{a}$, one of the free surface in the form of a "thumbnail" type flaw and one in the form of a "penny" shaped flaw embedded in the matrix of an inner 90° lamina as shown in figure 12. The stress intensity range, ΔK, for these two types of flaws are as follows:

Surface "Thumbnail" flaw [25]

$$\Delta K_{th} = 1.1\ \Delta\sigma_s\sqrt{\pi a}$$

where ΔK_{th} is the threshold stress intensity range, below which no crack growth will occur, and $\Delta\sigma_s$ is the corresponding threshold stress;

Embedded "Penny" shape flaw [26]

$$\Delta K_{th} = \frac{2\ \Delta\sigma_e\sqrt{a}}{\sqrt{\pi}} .$$

The above equations were solved for the threshold stress ratio to obtain

$$\frac{\Delta\sigma_e}{\Delta\sigma_s} = \frac{\dfrac{\Delta K_{th}}{2\sqrt{a}}}{\dfrac{\Delta K_{th}}{1.1\ \sqrt{\pi a}}} = 1.73$$

This implies that the stress required to grow an embedded flaw in the inner 90° lamina is 1.73 greater than the stress required to grow a surface flaw of the same size. Thus a $[90/0]_{2s}$ laminate would develop fatigue damage at a lower stress in the outer ply then a $[0/90]_{2s}$ laminate, in the inner ply. This explanation, which pertains to homogeneous isotropic materials, is not intended to

apply rigorously to the composites in question, since they are anisotropic in nature, but to suggest a qualitative trend.

In summary, it appears that the crack initiations on the free surface have little effect if the 0° fibers are on the outer plies due to the crack arresting capabilities of the fibers. In this case, the cracks initiate within the inner, off-axis lamina matrix. However, if off-axis plies (such as 90°) are on the outside, surface flaws may grow at stresses lower than those predicted from shakedown. Results similar to those discussed in this section were found for $[0/\pm 45/90]_s$ and $[90/\pm 45/0]_s$ laminates [13].

LOAD HISTORY EFFECT

Three $[0/\pm 45/90/0/\pm 45/\overline{90}]_s$ specimens were subjected to simple load variations; the corresponding fatigue damage in terms of unloading elastic modulus loss was monitored. Figure 13 presents results from a single specimen tested at $R = 0.1$ when S_{max} was increased stepwise. The cycling at a given level was continued until a relatively stable value of damage was reached (i.e., no significant drop in modulus with additional cycling). For reference, the data previously presented in figure 5 are shown as dashed lines in figure 13. The test was first conducted at maximum stress (S_{max}) equal 210 MPa; this resulted in a modulus drop to about 97 percent. This loss seems to be consistent with the dashed line for 225 MPa. The S_{max} was then raised to 275 MPa, which resulted in a loss to

about 73 percent (slightly lower than the dashed 275 MPa data). The test specimen was then subjected to S_{max} = 337 MPa which caused further drop in modulus to about 58 percent, which is slightly above the dashed line for 350 MPa. The test results of figure 13 imply that a laminate will seek the SDS associated with the current value of S_{max} if S_{max} is the largest in the loading history.

The response of a laminate subjected to a constant stress range (i.e., 225 MPa), but with varying values of S_{max} was investigated. Figure 14 indicates that the modulus drops when the S_{max} is shifted upward. As expected, the modulus did not decrease when S_{max} was lowered from 325 to 275 MPa.

Figure 15 presents additional data. Again the stress range was constant (ΔS = 225 MPa) (until the last loading segment). The shift from S_{max} = 325 to 300 MPa resulted in a gradual modulus decrease of approximately 2 percent. The 300 to 325 MPa shift upward in figure 14 resulted in an over 4 percent drop. No detectable damage was created by decreasing S_{max} = 300 to 250 MPa. The S_{max} was then increased to 325 MPa and additional damage resulted. Finally, this maximum stress was then held at 325 MPa and the stress range increased such that R = 0.1. The damage resulted in a modulus loss of approximately 36 percent which is close to what one might expect from figure 5.

From observations of these three tests, two phenomena seem obvious:

(1) For a given stress ratio, the specimen seeks the SDS for the largest S_{max} to which it is subjected. The simple damage accumulation model in figure 8 may be used to give a possible explanation of this phenomenon. An increase in the cyclic stress range above the shakedown range must result in an increase in the amount of matrix fatigue damage to re-establish a new saturation damage state. Once the new saturation damage state is established, reducing the stress range within the ΔS range on figure 9 will clearly result in no additional damage.

(2) For a constant stress range, relatively negligible modulus drop is generated by shifting the mean stress downward, whereas significant loss may be created by shifting the mean stress upward. This second phenomenon is attributed to the tensile plastic deformation and the opening and extension of the existing cracks during the upward shift of the stress range. The previously presented model, figures 8 and 9, does not account for this drop in modulus due to increasing the mean stress. It is clear, however, from figure 8 that a downward shift of the stress range would result in a compressive yielding of the matrix which would not serve to open or extend the present cracks further. Thus, raising the cyclic mean stress would be more damaging than lowering.

Although the variable load history tests were simple, they revealed some interesting implications for fatigue response under

complex spectrum loads. For example, Miner's cumulative damage would not apply for the no-fatigue-damage region. For constant amplitude tests the fatigue damage was found to be a function of stress range, but not mean stress. However, if one were to use the shakedown stress range and randomly change the mean, fatigue damage would result from the plastic deformation required each time the mean was shifted. In this manner it is not so much the cyclic load causing the damage as the plastic excursion between cyclic levels.

CONCLUDING REMARKS

A shakedown analysis for annealed matrix, metal matrix composites was shown to predict the stress amplitude below which no fatigue damage accumulated in laminate with 0° fibers on the outside.

A simple fatigue damage accumulation analysis was presented which adequately described the relationship between matrix modulus drop due to matrix fatigue cracks and overall laminate properties. A method for predicting changes in the laminate properties was developed. It is based upon a model that envisions a saturation damage state to be able to exist during constant amplitude fatigue loading.

Data were presented to show the difference in fatigue response of laminates that differed only in stacking sequence; are laminate had 0° plies on the surface whereas the other had 90° plies on the outside surface. The 90° plies on the surface developed cracks earlier than predicted by shakedown. An attempt was made to predict this stacking sequence effect.

Variable load history effects on the fatigue damage response were investigated by simple tests. These tests revealed that, for a given stress ratio, the specimen seeks the saturation damage state for the largest stress range to which it is subjected. It was also found that relatively negligible modulus loss results when shifting a given cyclic stress range down, whereas significant damage may be created by shifting upward.

ACKNOWLEDGMENT

This work was conducted primarily at Duke University under the supervision of Professor George Dvorak, presently at the University of Utah, and sponsored by the Army Research Office. The C-scan equipment at Virginia Polytechnic Institute and State University was used for the ultrasonic inspections.

APPENDIX

SCREENING OF COMPOSITE LAMINATES USING ULTRASONIC C-SCANS

Typically, fatigue test data results are quite scattered. Most of this scatter is due to material variability. One specimen may contain more, or different, microscopic (or macroscopic) defects than another. This problem is even more prevalent in composite materials than in metals. Defects, in addition to those that exist in metals, that occur in composites are nonuniform fiber spacing, weak fiber-matrix interfaces, and interlaminar debonds. These defects may differ not only from one composite laminate to another, but also between locations within the single laminate from which the test specimens were cut. It is therefore desirable to have a nondestructive evaluation (NDE) technique that will screen the specimens for "quality."

Davis and Sullivan [28] and Knott and Stinchcomb [29] discussed some of the current advances and problems concerning the nondestructive inspection of composite materials. Chang, Gordon, and Gardner [30] studied fatigue damage in composites by means of various nondestructive techniques. Presently, one of the most common NDE techniques for detecting flaws in composites is the ultrasonic C-scan.

The C-scan NDE technique is a special case of ultrasonics. McGonnagle [31] presents a detailed discussion on the various NDE techniques which includes the ultrasonic C-scan. Basically, the ultrasonic technique propagates sound waves through the material being evaluated.

The wave response can be interpreted to detect material variations. Material variations such as density, voids, and delaminations create different responses in the wave propagation which can be distinguished from the response created by a defect-free area.

The C-scan is analogous to a two-dimensional photograph; it is a projection of the internal details of the specimen onto a plane. Thus, the C-scan gives the shape and location of the internal defects in a plane parallel to the surface. The depth of the defect is unknown.

The C-scan does not indicate the physical nature of the defect, nor does it indicate how strongly the defect might influence the static strength or fatigue life. These properties can only be correlated with the observed defects.

To correlate C-scans with fatigue response, annealed boron-aluminum 6061-0 $[0/\pm45/90/0/\pm45/\overline{90}]_s$ composite specimens were tested. A large 15-layer laminate was cut into rectangular specimens, each 10.16 cm long and 1.27 cm wide. The specimens were C-scanned. These scans were rated to designate the specimen as "good" (G), "defective" (D), or "very defective" (VD), according to the relative amount of defect indications as shown in Figure 16.

Presented in Figure 17 are fatigue S-N curve data points designated as G, D, or VD. The "good" specimens have a fatigue limit of 375 MPa (at 2×10^6 cycles) compared to 338 MPa for the "defective" specimen. These data suggest that only one serious flaw need be present to drastically truncate the fatigue life. It is difficult to

infer the fatigue response of a given laminate from its C-scan indications. However, the greater the number of flaws indicated, the more likely is the occurrence of a severe flaw. As might be expected, the VD specimen resulted in a relatively short fatigue life.

Below each of the C-scans in Figure 16, the maximum stress level for its fatigue test is given. The fracture location is also indicated for each specimen by a line drawn on either side of the C-scan. Notice that the fracture sites seem to coincide with defect locations if defects are present. (Doublers, approximately 3.2 cm long, were bonded to the ends of the specimen making the defects in this area of little consequence.)

Many of the defects in the "defective" specimens of Figure 16 are narrow, clearly defined, and are oriented 0°, 45°, or 90° to the axial direction. These defects were found to be missing fibers due to poor fiber spacing during fabrication. Figure 18 is a photograph of a specimen's edge showing several missing fibers in the 45° lamina, as was indicated in the C-scan. These types of defects would serve to make the area locally weak, allowing earlier and more extensive fatigue damage to the matrix, and causing an early failure in that area.

The reduction in elastic unloading modulus [12,13] versus the number of cycles has been shown to depend on specimen quality. Since the elastic modulus is measured in a global manner over a 2.54 cm gage section, small areas of local weakness, such as missing fibers, may not degrade the elastic modulus in a noticeable fashion. However, a

specimen in the "very defective" category should show a noticeable decrease in the elastic modulus. Notice in Figure 19 that at approximately the same stress level, there is little difference between the G and D specimen until just before failure. As expected, the VD specimen had a rapid decrease in modulus and a short fatigue life, despite its lower stress level.

In summary, it has been shown that those specimens with a higher defect density suffer relatively more rapid fatigue damage. It would be difficult to define an accurate "degree of defect" by the C-scan examination. One can, however, identify a "good" (no obvious defects) specimen with some confidence. Therefore, the C-scan can be used to screen specimens to identify the "good" specimens or the best of the available specimens for testing and evaluation purposes.

REFERENCES

[1] Baker, A. A., "The Fatigue of Fibre-Reinforced Aluminum," Journal of Materials Science, Vol. 3, 1968, pp. 412-423.

[2] Baker, A. A., Braddick, D. M., and Jackson, P. W., "Fatigue of Boron-Aluminum and Carbon Aluminum Fibre Composites," Journal of Materials Science, Vol. 7, 1972, pp. 747-762.

[3] Jackson, P. W., Baker, A. A., and Braddick, D. M., "Some Aspects of the Fracture of Boron-Aluminum Composites," Journal of Materials Science, Vol. 6, 1971, pp. 427-438.

[4] Shimizu, H., and Dolowy, J. F., Jr., "Fatigue Testing and Thermal-Mechanical Treatment Effects on Aluminum-Boron Composites," ASTM STP 460, American Society for Testing and Materials, 1969, pp. 192-202.

[5] Hancock, J. R., "Fatigue of Metal-Matrix Composites," Composite Materials, Vol. 5, Fracture and Fatigue, Edited by Broutman, Academic Press, 1974.

[6] Toth, I. J., "Creep and Fatigue Behavior of Unidirectional and Cross-Plied Composites," ASTM STP 460, American Society for Testing and Materials, 1969, pp. 236-253.

[7] Menke, G. D., and Toth, I. J., "The Time Dependent Mechanical Behavior of Metal Matrix Composites," AFML-TR-71-102, Air Force Materials Laboratory, September 1971.

[8] Christian, J. L., "Axial Fatigue Properties of Metal Matrix Composites," ASTM STP 569, American Society for Testing and Materials, 1975, pp. 280-294.

[9] Gouda, M., Prewo, K. M., and McEvily, A. J., "On the Mechanics of Fatigue in Boron-Aluminum Composites," to appear in ASTM STP 723, American Society for Testing and Materials.

[10] White, M. K., and Wright, M. A., "The Fatigue Properties of Cross-Plied Boron 6061 Aluminum," Journal of Materials Science, Vol. 14, 1979, pp. 653-662.

[11] Stinchcomb, W. W., Reifsnider, K. L., Marcus, L. A., and Williams, R. S., "Effects of Frequency on the Mechanical Response of Two Composite Materials to Fatigue Loading," ASTM STP 569, American Society for Testing and Materials, 1976, pp. 115-129.

[12] Dvorak, G. J., and Johnson, W. S., "Fatigue of Metal Matrix Composites," to appear in International Journal of Fracture.

[13] Johnson, W. S., "Characterization of Fatigue Damage Mechanisms in Continuous Fiber Reinforced Metal Matrix Composites," Ph.D. Dissertation, Duke University, December 1979.

[14] Dvorak, G. J., and Tarn, J. Q., "Fatigue and Shakedown in Metal Matrix Composites," ASTM STP 569, American Society for Testing and Materials, 1975, pp. 145-168.

[15] Aluminum, Vol. 1, K. R. VanHorn, Ed., American Society for Metals, Metals Pack, Ohio, 1967, p. 183.

[16] Melan, E., "Zur Plastizität des Räumlichen Kontinuums," Ingenieur-Arch, Vol. 9, 1938, p. 116.

[17] Symonds, P. S., "Shakedown in Continuous Media," J. Appl. Mech., Vol. 18, 1951, p. 85.

[18] Maier, G., "Shakedown Theory in Perfect Elastoplasticity with Associated and Nonassociated Flow Laws: A Finite Element, Linear Programming Approach," Meccanica 4, 1969, p. 250.

[19] Koiter, W. T., "A New General Theorem on Shakedown of Elastic-Plastic Structures," Proc. Koninkl. Nederl. Akad. van Wetenschappen, Amsterdam, Series B59, No. 1, 1956, p. 24.

[20] Tarn, J. Q., Dvorak, G. J., and Rao, M. S. M., International J. of Solids and Structures, Vol. 11, 1975, pp. 751-764.

[21] Dvorak, G. J., Rao, M. S. M., and Tarn, J. Q., J. of Appl. Mech., Vol. 4, 1974, pp. 249-253.

[22] Dvorak, G. J., and Bahei-El-Din, Y. A., "Plasticity of Composite Laminates," Proc. of Research Workshop on Mechanics of Composite Materials, Duke University, October 17-18, 1978.

[23] Bahei-El-Din, Y. A., and Dvorak, G. J., "Plastic Yielding at a Circular Hole in a Laminated FP-Aℓ Plate," in Modern Developments in Composite Materials and Structures, J. R. Vinson, Ed., ASME, New York, 1979, pp. 123-147.

[24] Bahei-El-Din, Y. A., "Plastic Analysis of Metal-Matrix Composite Laminates," Ph.D. Dissertation, Duke University, July 1979.

[25] Johnson, W. S., "Prediction of Constant Amplitude Fatigue Crack Propagation in Surface Flaws," ASTM STP 687, American Society for Testing and Materials, 1979, pp. 143-155.

[26] Tada, H., Paris, P. C., and Irwin, G. R., The Stress Analysis of Cracks Handbook, Del Research Corporation, Hellertown, Pennsylvania, 1973, p. 24.1.

[27] Mayfield, Jerry, "New Fibers Developed for Composites," Aviation Week and Space Technology, January 8, 1979, pp. 35-41.

[28] Davis, L. W., and Sullivan, P. G., "Nondestructive Evaluation," Summary of the Proc. of the Second Conference on Carbon Fiber Reinforced Metal Matrix Composites, Monterey, California, May 1978.

[29] Knott, M. A., and Stinchcomb, W. W., "Non-Destructive Evaluation of Fatigue Damage in Boron-Aluminum Composites with Initial Defects," Proc. of the 12th Symposium on Non-Destructive Evaluation, Southwest Research Institute, San Antonio, Texas, April 1979.

[30] Chang, F. H., Gordon, D. E., and Gardner, A. H., "A Study of Fatigue Damage in Composites by Nondestructive Testing Techniques," Fatigue of Filamentary Composites, ASTM STP 636, American Society for Testing and Materials, 1977, pp. 57-72.

[31] McGonnagle, W. J., Nondestructive Testing, Second Ed., Gordon and Breach, New York, 1961.

TABLE 1.- COMPOSITE CONSTITUENTS MECHANICAL PROPERTIES

	Boron fiber [27] 0.142 mm diameter	6061 Aluminum
Elastic modulus	$E^f = 40.0 \times 10^4$ MPa $(58.0 \times 10^6$ psi)	$E^m = 7.25 \times 10^4$ MPa $(10.5 \times 10^6$ psi)
Poisson's ratio	$\nu^f = 0.200$	$\nu^m = 0.33$

TABLE 2.- PREDICTED AND EXPERIMENTAL LAMINATED COMPOSITE BEHAVIOR

Layup	V_f	$E_o \times 10^5$ MPa	$\Delta S_{sh}/Y$	Shakedown stress range, ΔS_{sh}		$\Delta S_R^{\phi}/\Delta S_{sh}$
				Pred.	Exp.	
$[0]_8$	0.45	2.200	6.10	429	481	1.12
$[0/90]_{2s}$	0.50	1.840	3.13	220	214	0.97
$[90/0]_{2s}$	0.50	1.840	3.13	220	173	0.79
$[0/\pm45/90]_s$	0.33	1.264	2.60	183	166	0.91
$[90/\pm45/0]_s$	0.30	1.210	2.57	181	123	0.68
$[0/\pm45/90/0/\pm45/\overline{90}]_s$	0.45	1.514	2.71	191	196	1.03

TABLE 3.- SATURATION DAMAGE STATE PREDICTIONS

Layup	S_{max} MPa	R	$\Delta\varepsilon \times 10^{-3}$	E_{Al}^{eff} MPa	E_N/E_o	
					Predicted	Experimental
$[0]_8$	900	0.3	2.96	36,653	91	96
	800	0.1	3.40	29,813	89	94
$[0/90]_{2s}$	450	0.1	2.88	24,410	71	63
	350	0.1	1.58	44,494	84	82
$[90/0]_{2s}$	450	0.1	3.60	17,826	67	66
	250	0.1	1.70	46,029	85	83
$[0/\pm45/90]_s$	225	0.1	2.10	47,954	79	76
	200	0.1	1.60	72,450	100	89
$[90/\pm45/0]_s$	180	0.1	1.70	39,287	70	75
	160	0.1	1.40	49,712	80	83
$[0/\pm45/90/0/\pm45/\overline{90}]_s$	350	0.1	3.7	22,802	42	51
	275	0.1	2.0	50,831	83	79

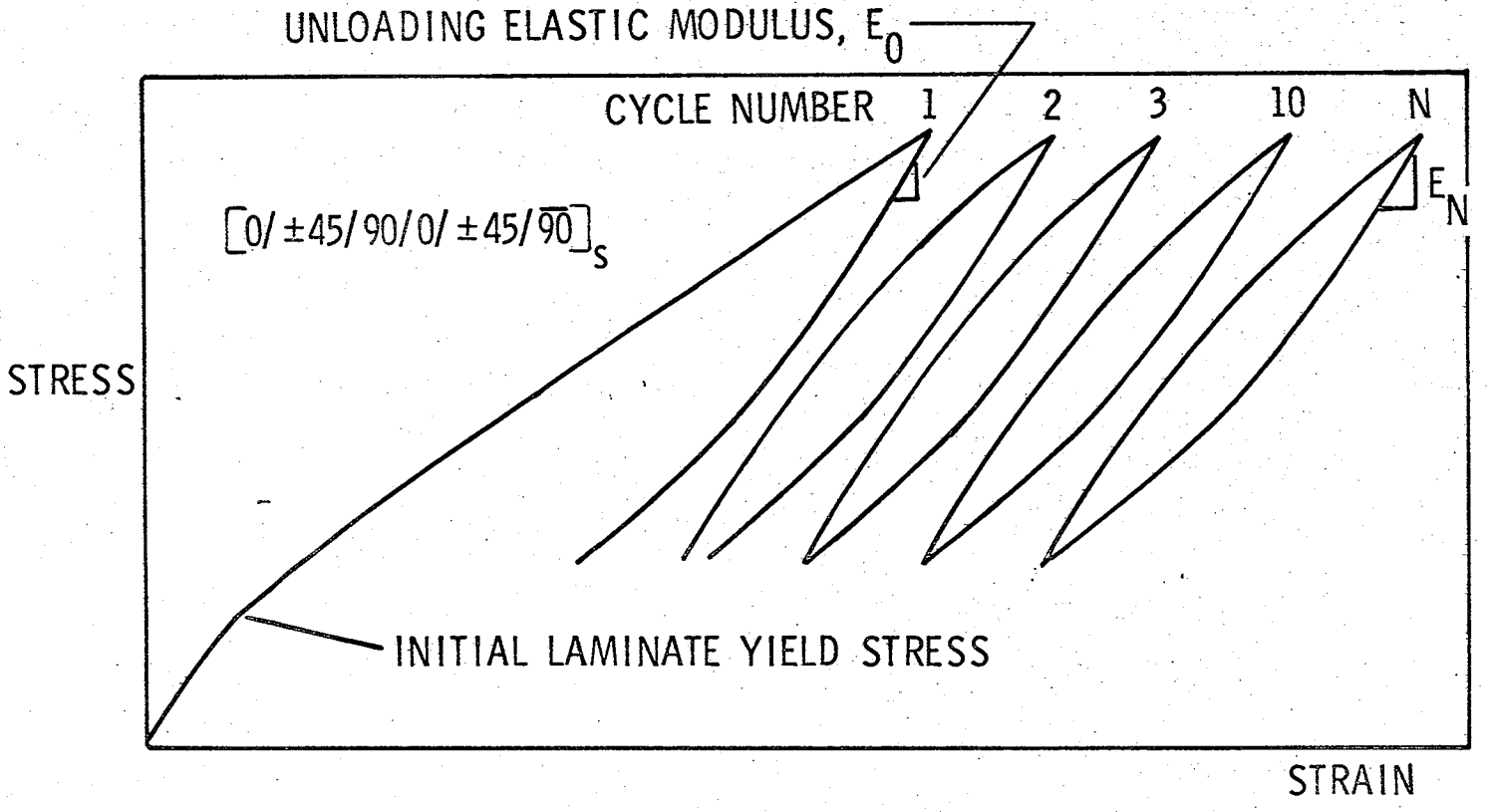

Figure 1.- Example stress-strain recording of a B/Al laminated composite specimen.

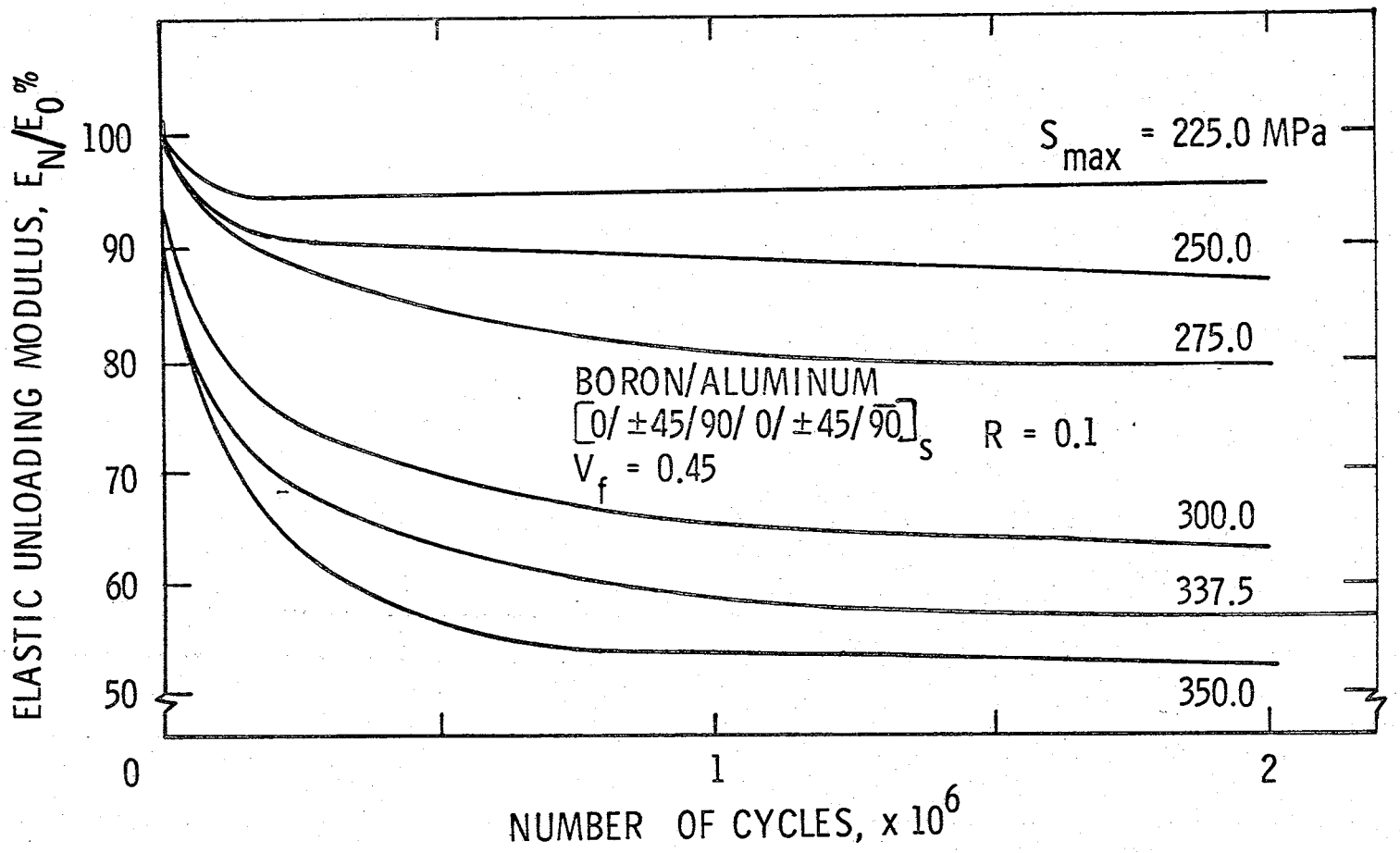

Figure 2.- Change in elastic modulus of $[0/\pm45/90/0/\pm45/\overline{90}]_S$. Specimens tested at different values of S_{max}.

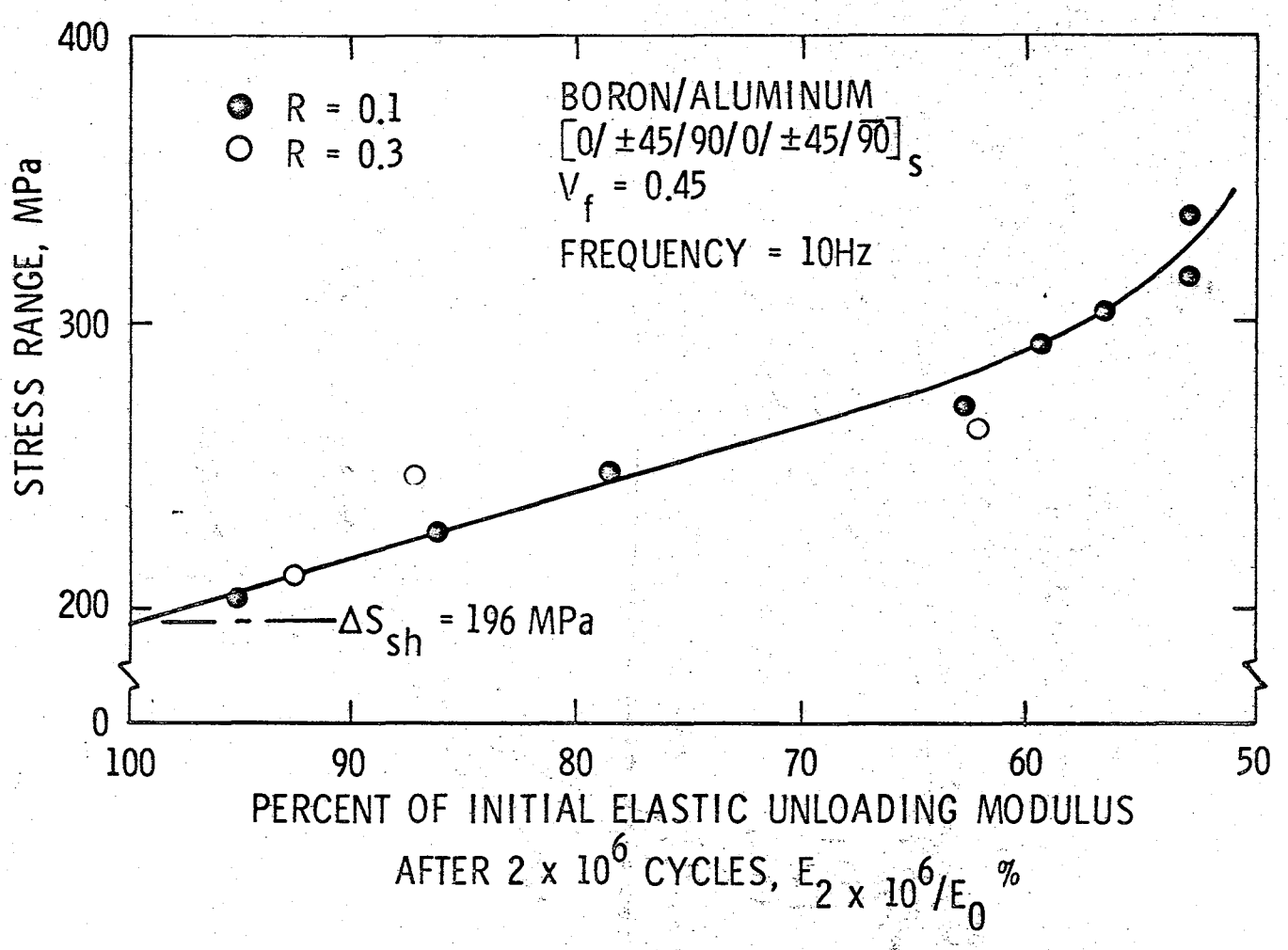

Figure 3.- Change in elastic modulus of $[0/\pm45/90/0/\pm45/\overline{90}]_s$. Specimens related to applied stress range ΔS.

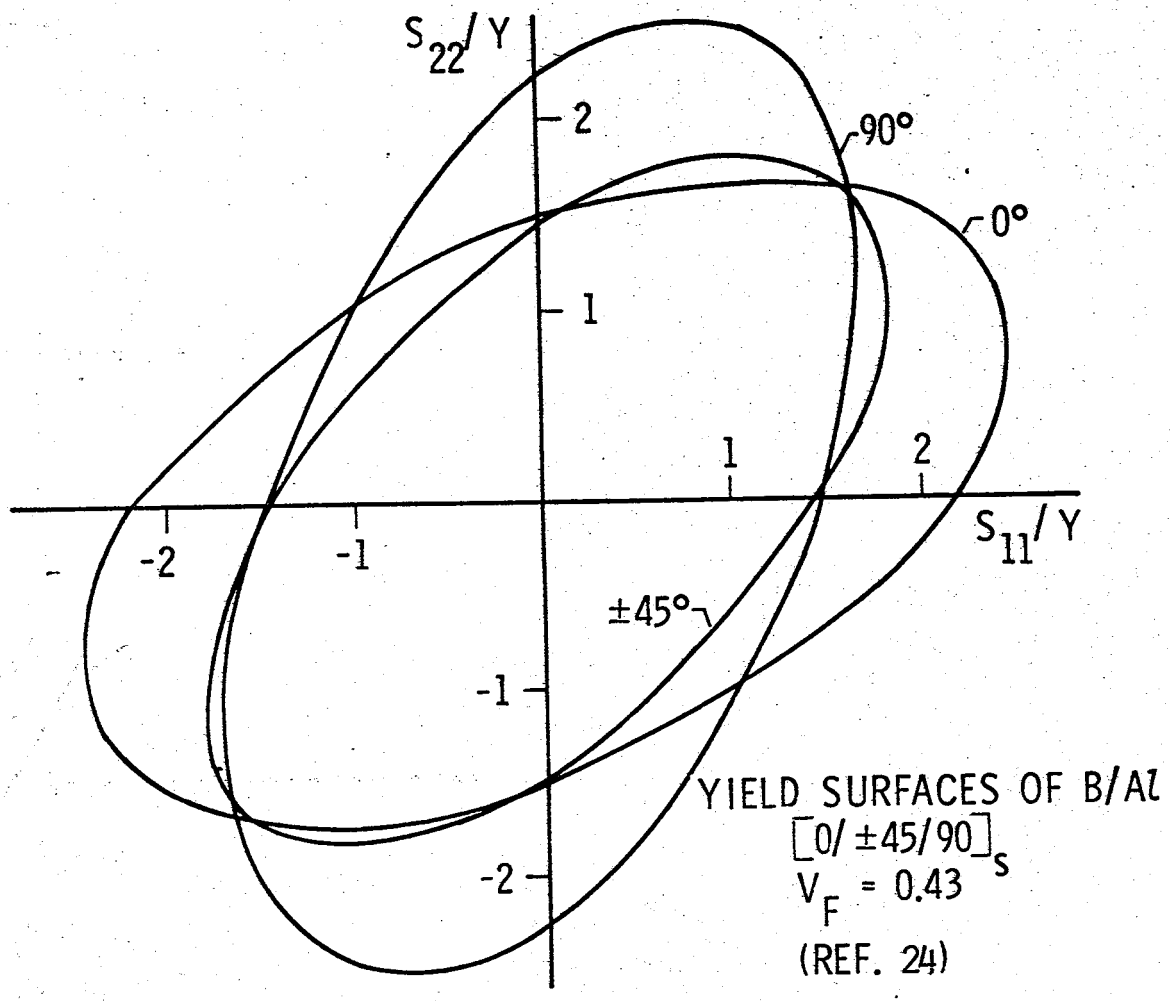

Figure 4.- Yield surfaces for plies of a B/Al laminate. The S_{11} direction coincides with 0^o fiber direction.

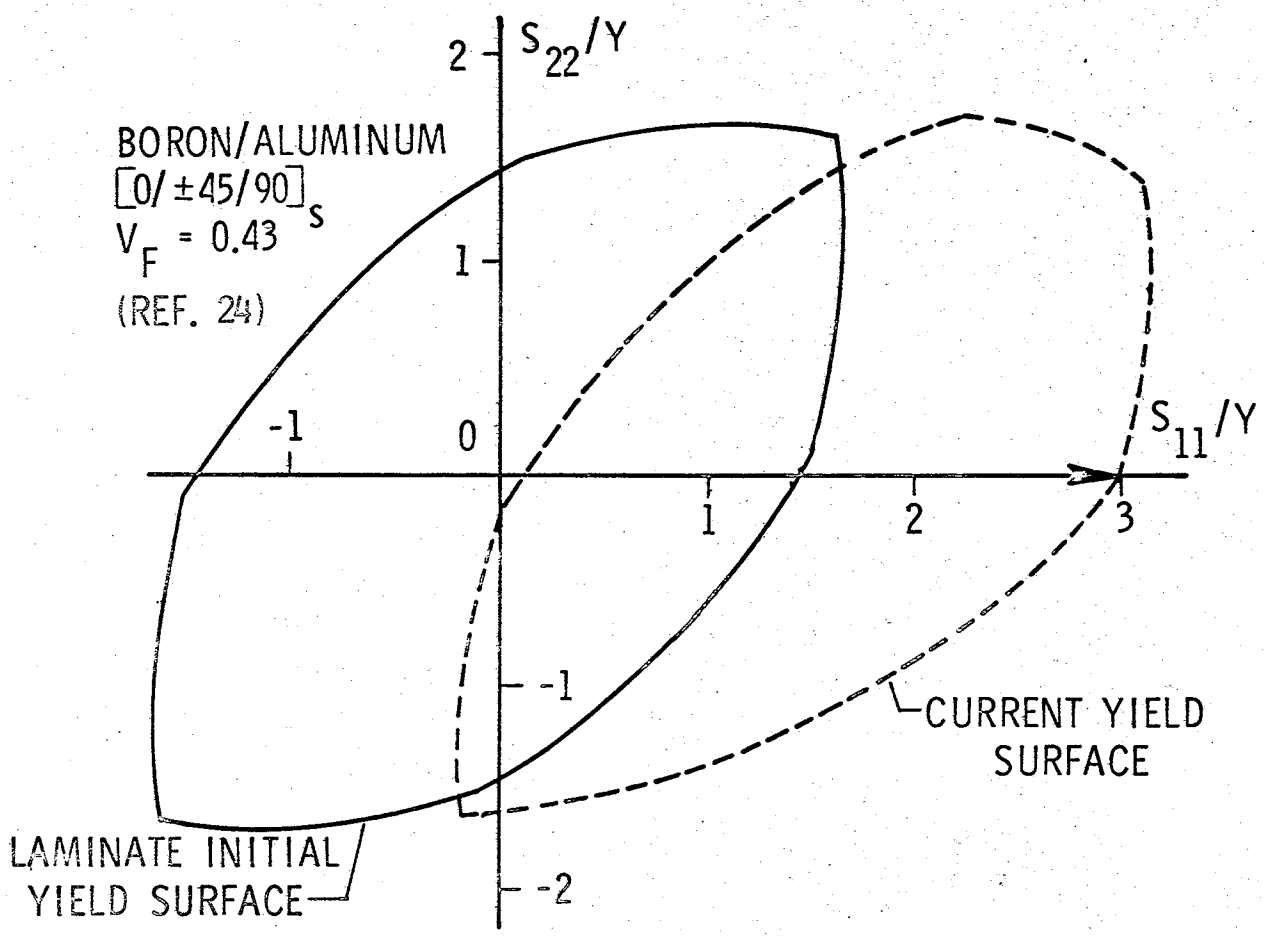

Figure 5.- Initial and current yield surfaces of a B/Al laminate. The S_{11} direction coincides with 0° fiber direction.

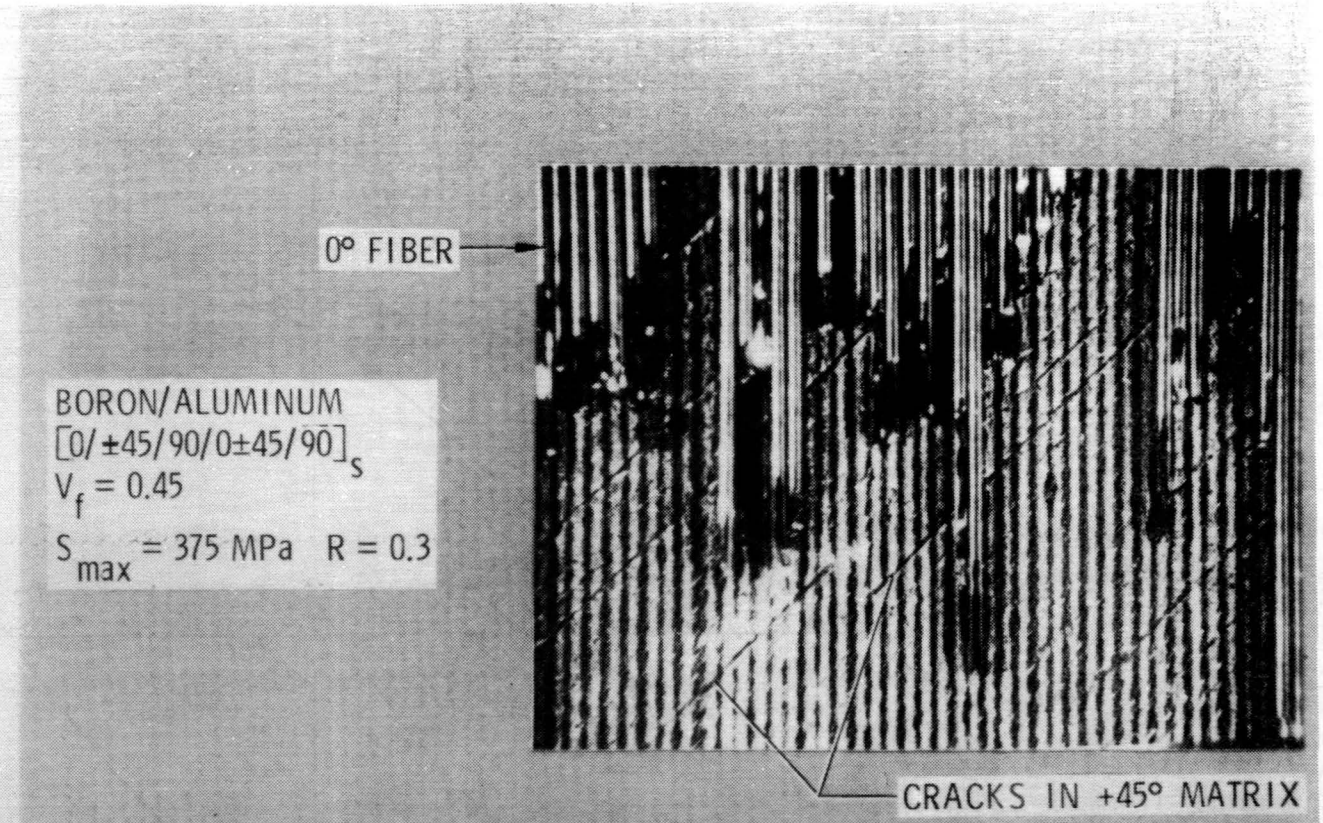

Figure 6.- Cracks in the +45° lamina matrix material.

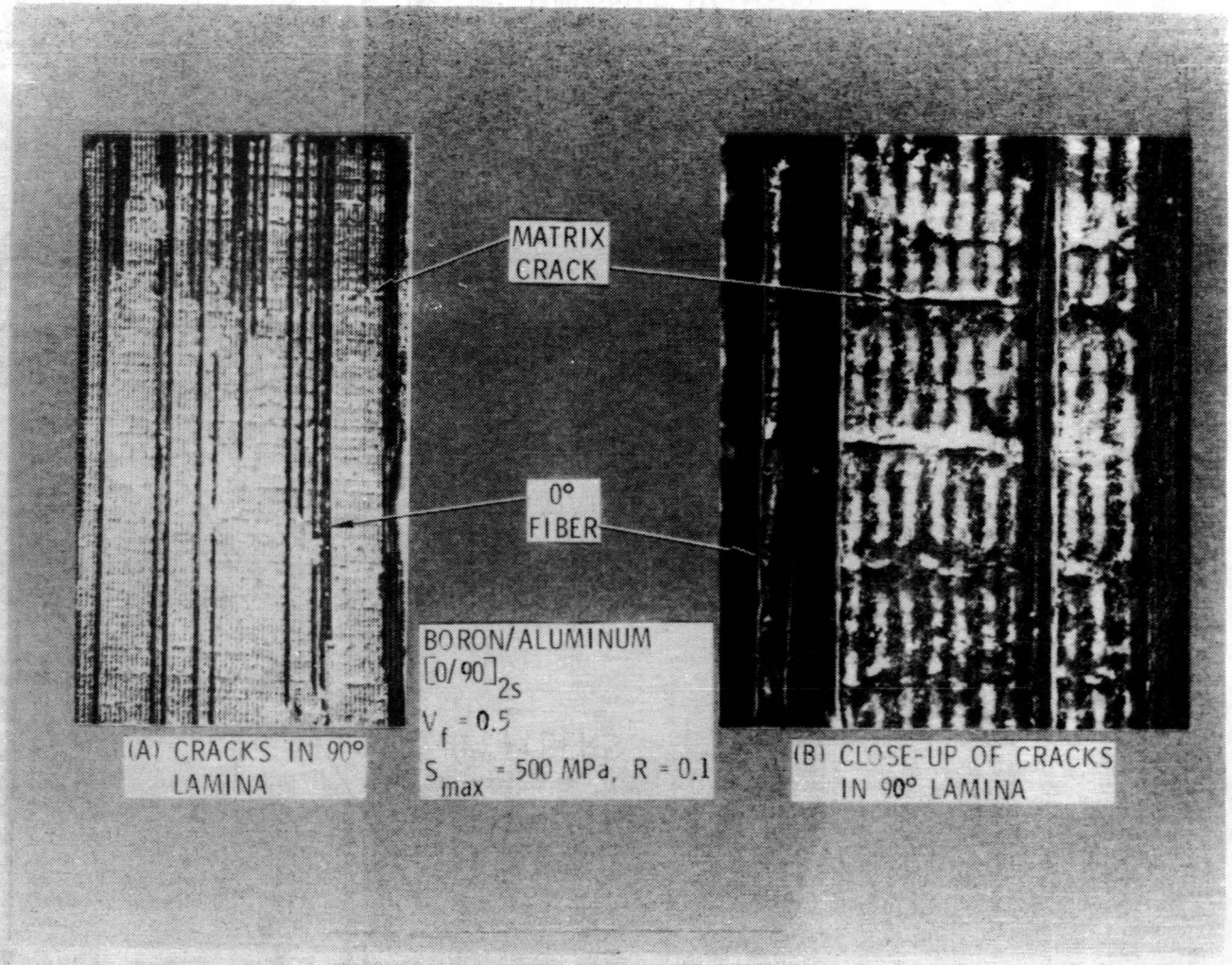

Figure 7.- Cracks in 90° lamina matrix material.

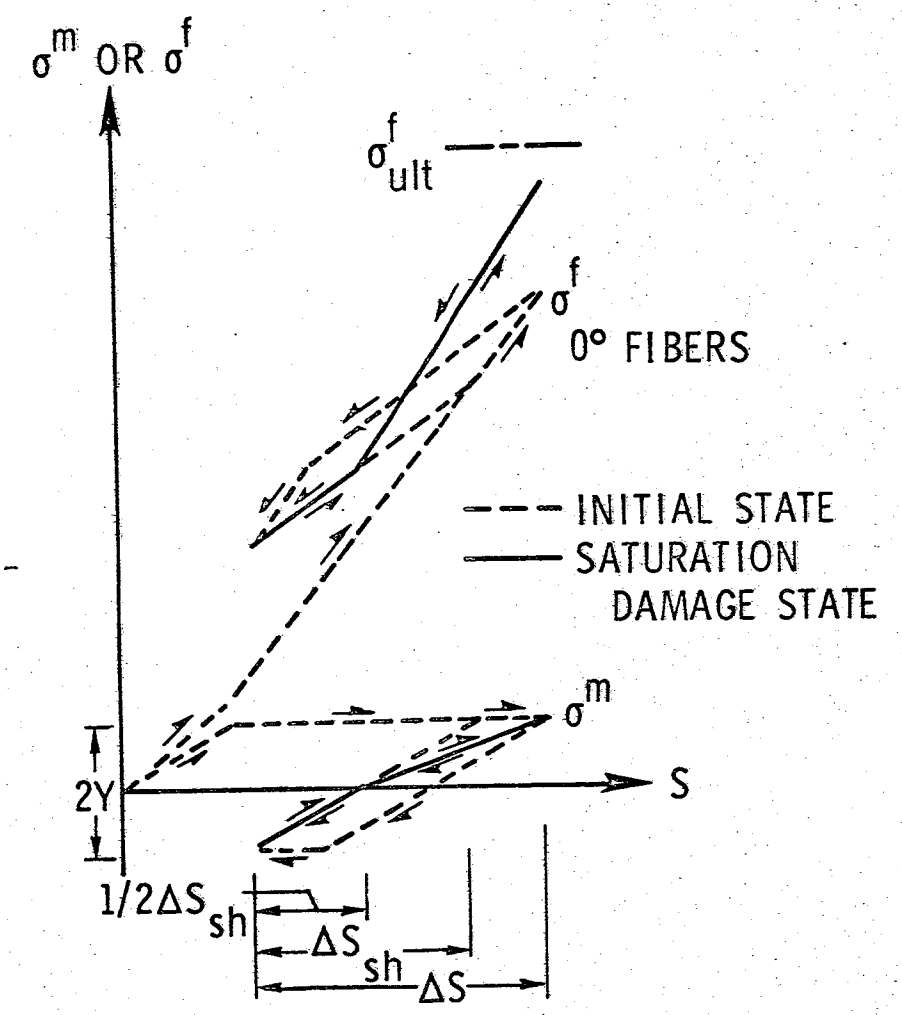

Figure 8.- Decreasing tensile matrix response and increasing 0^{o} fiber stress as the laminate attains a saturation damage state.

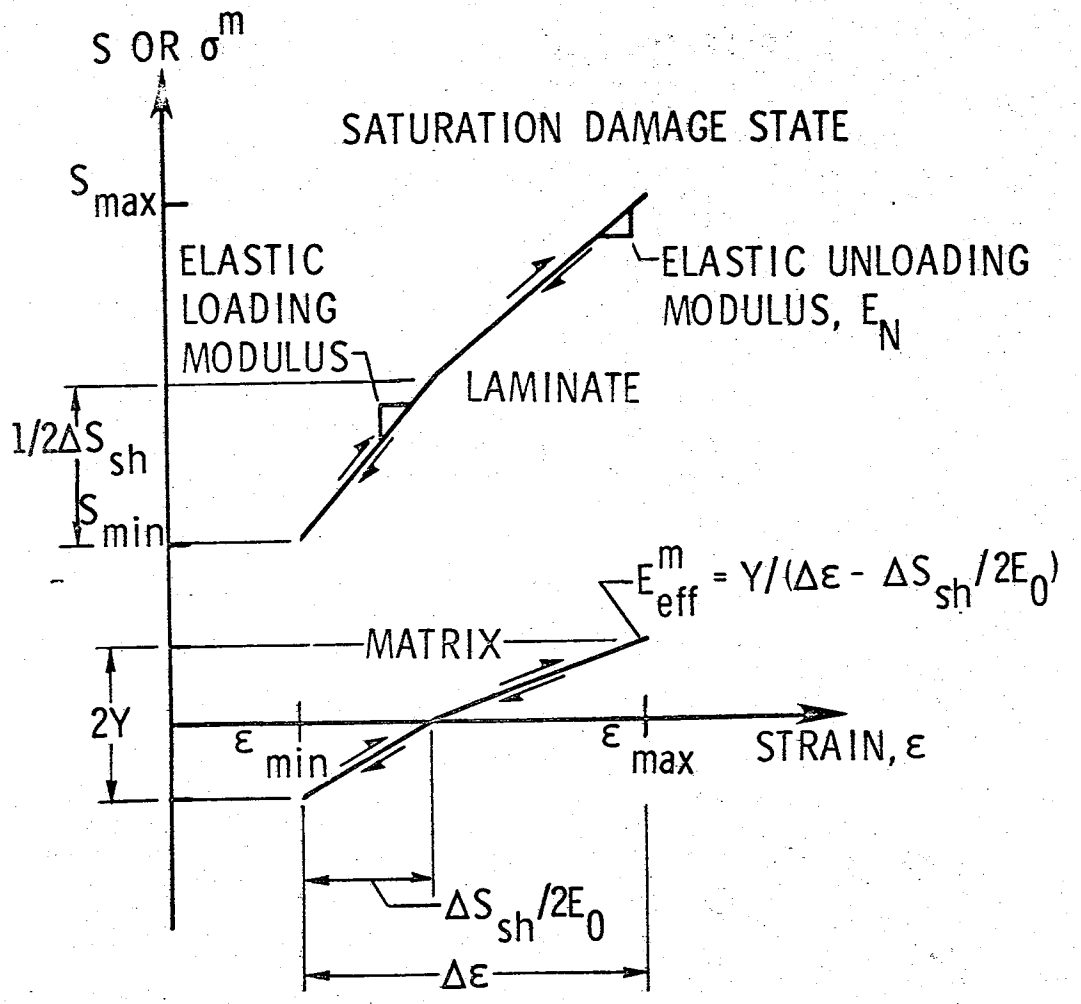

Figure 9.- Composite laminate and matrix stress-strain response for a saturation damage state.

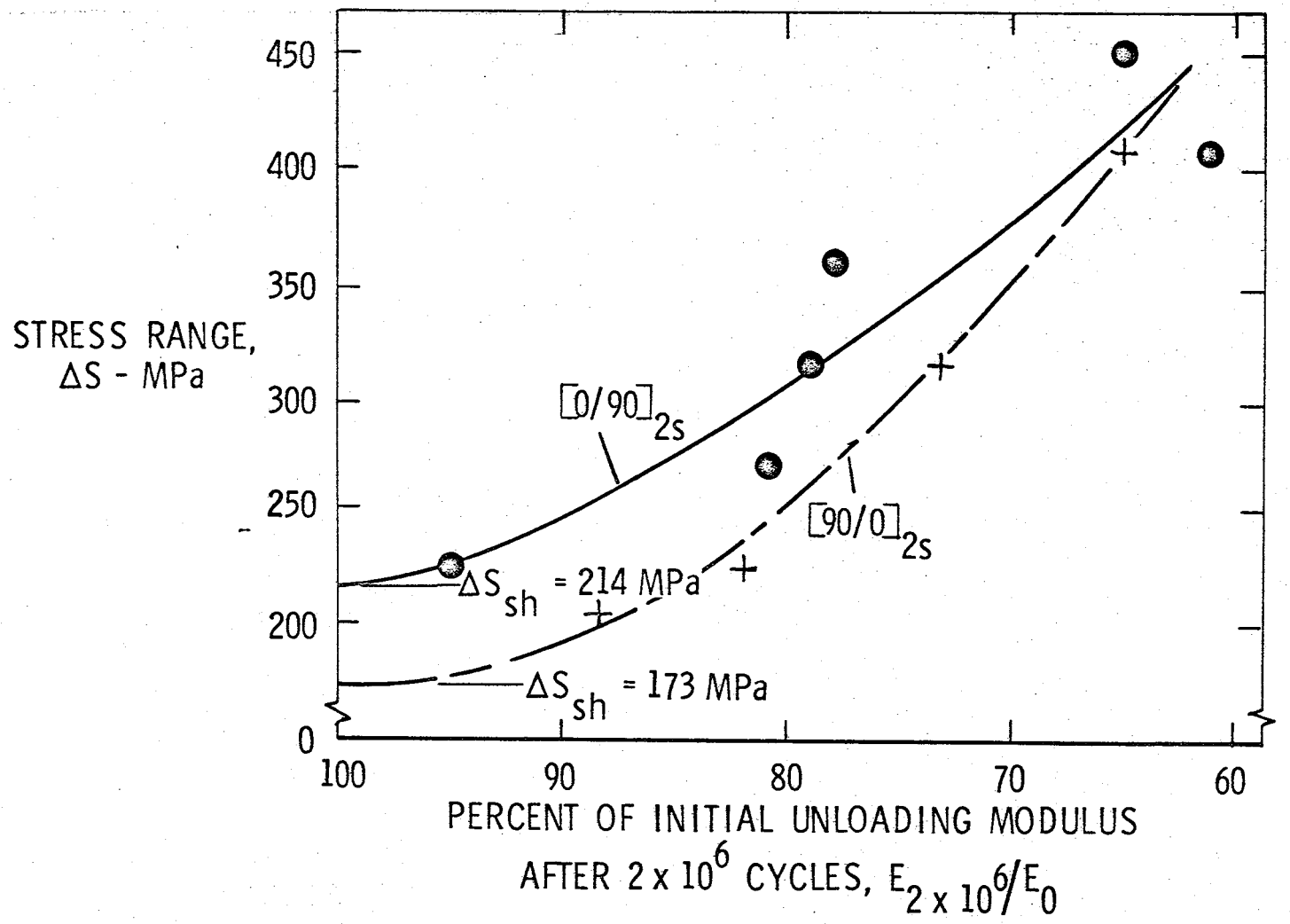

Figure 10.- Change in elastic unloading modulus of $[0/90]_{2s}$ and $[90/0]_{2s}$ specimens for a range of applied stress.

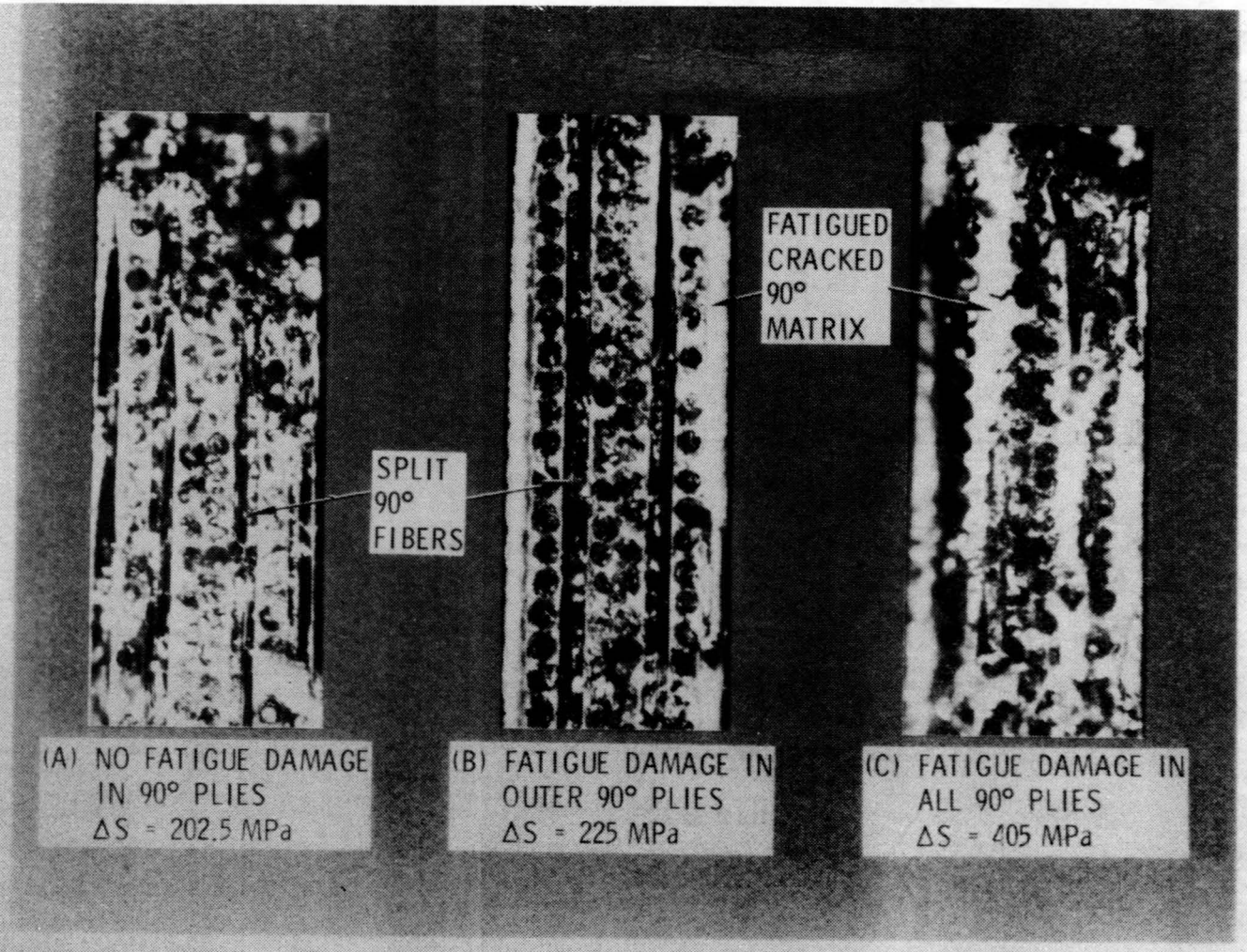

Figure 11.- Fracture surfaces indicating the degree of fatigue cracking present, $[90/0]_{2s}$, R = 0.1.

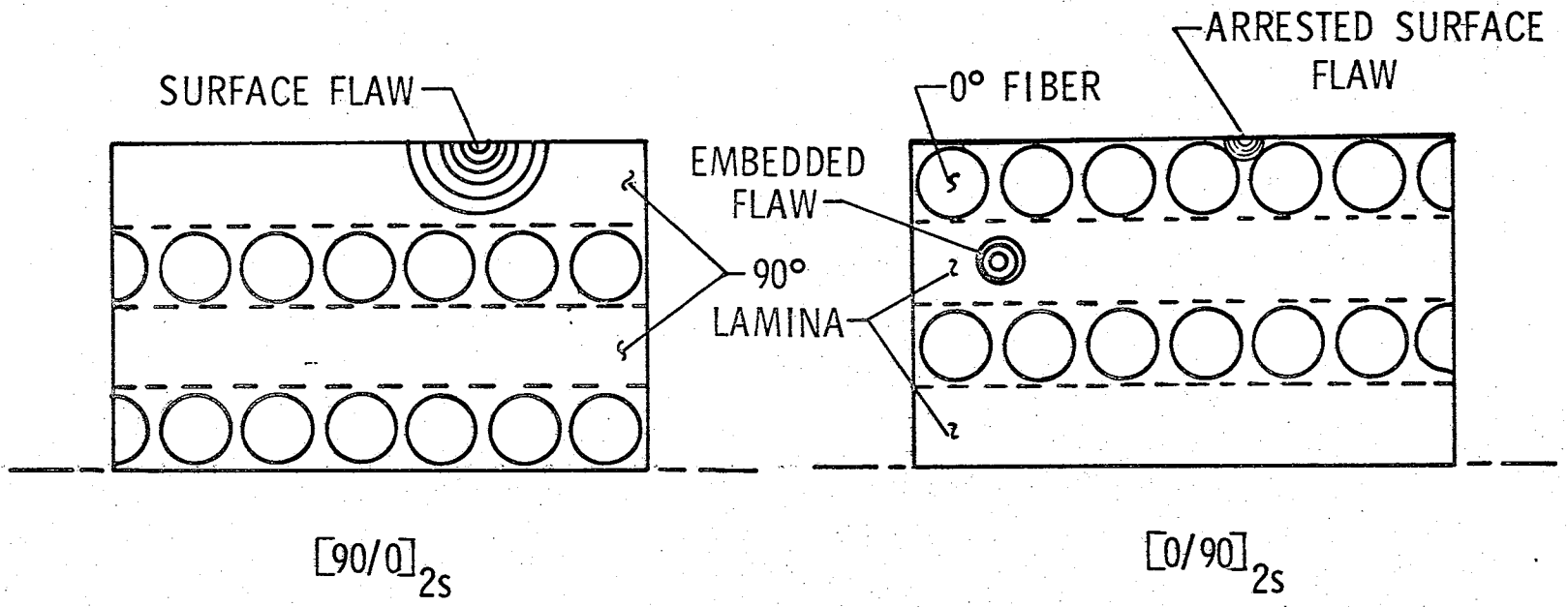

Figure 12.- Schematic of possible crack initiation sites.

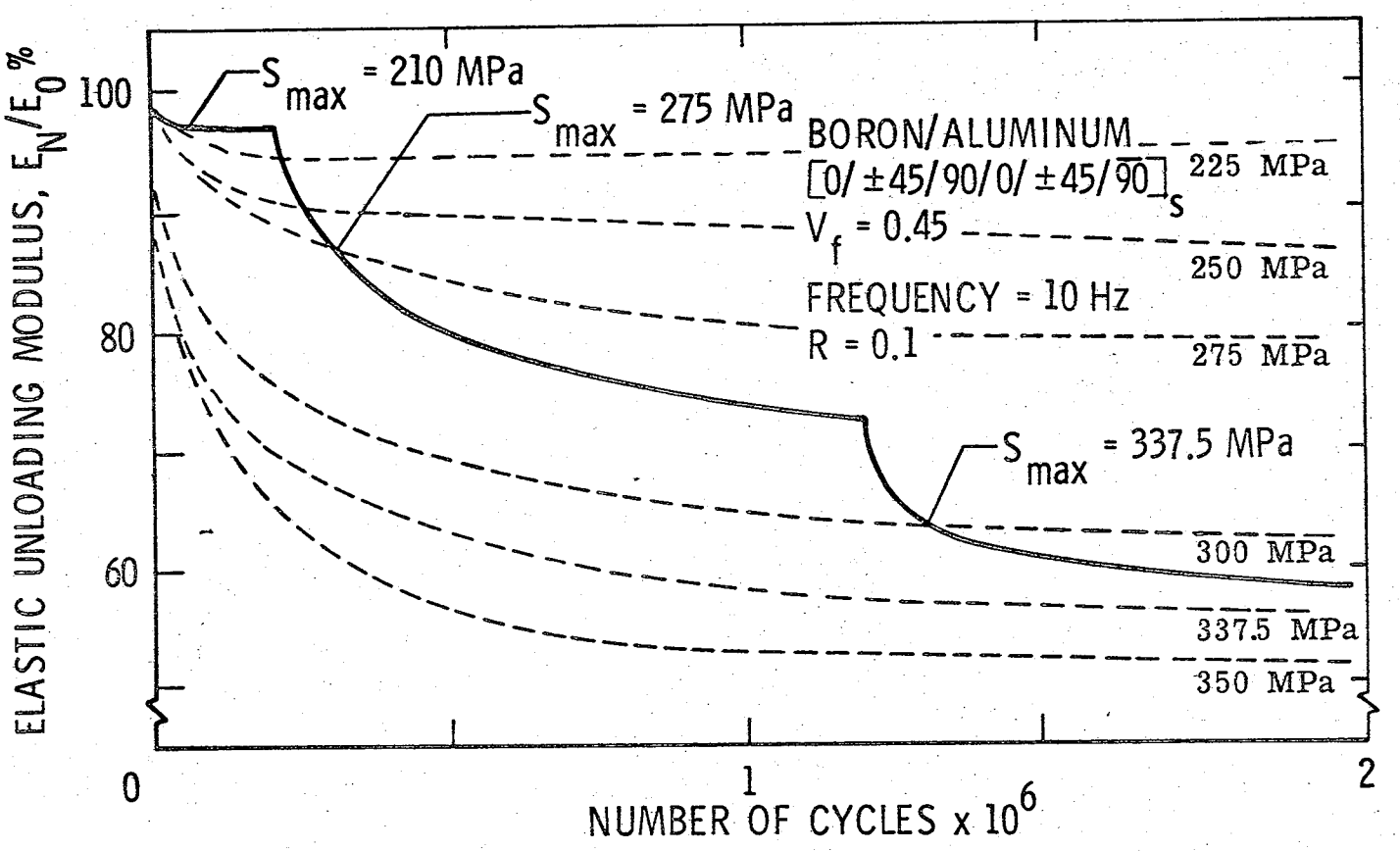

Figure 13.- Change in elastic unloading modulus of a $[0/\pm45/90/0/\pm45/\overline{90}]_s$ specimen with increasing S_{max} at a constant R = 0.1.

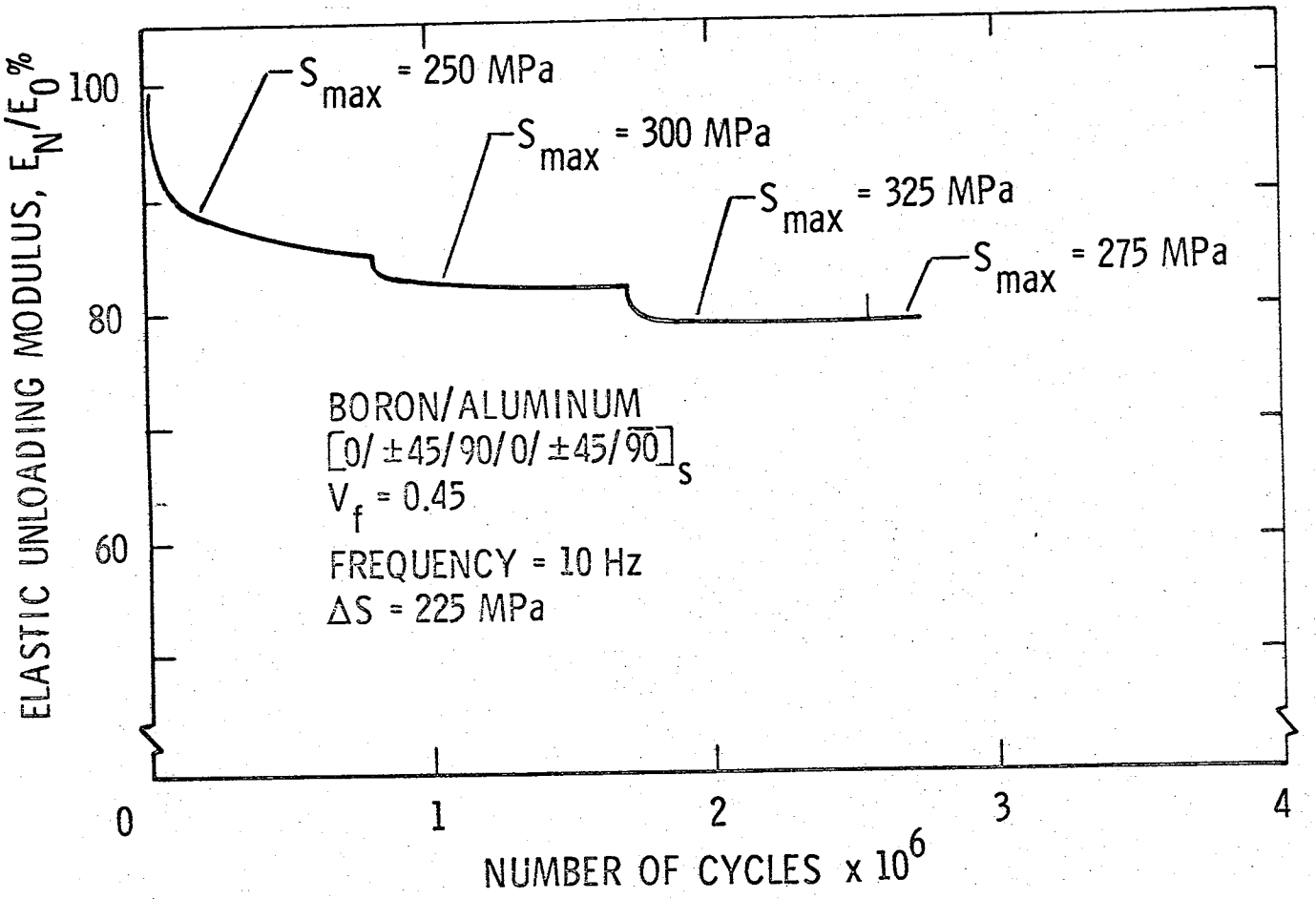

Figure 14.- Change in elastic unloading modulus under constant stress range and varying maximum stress (primarily increasing S_{max}).

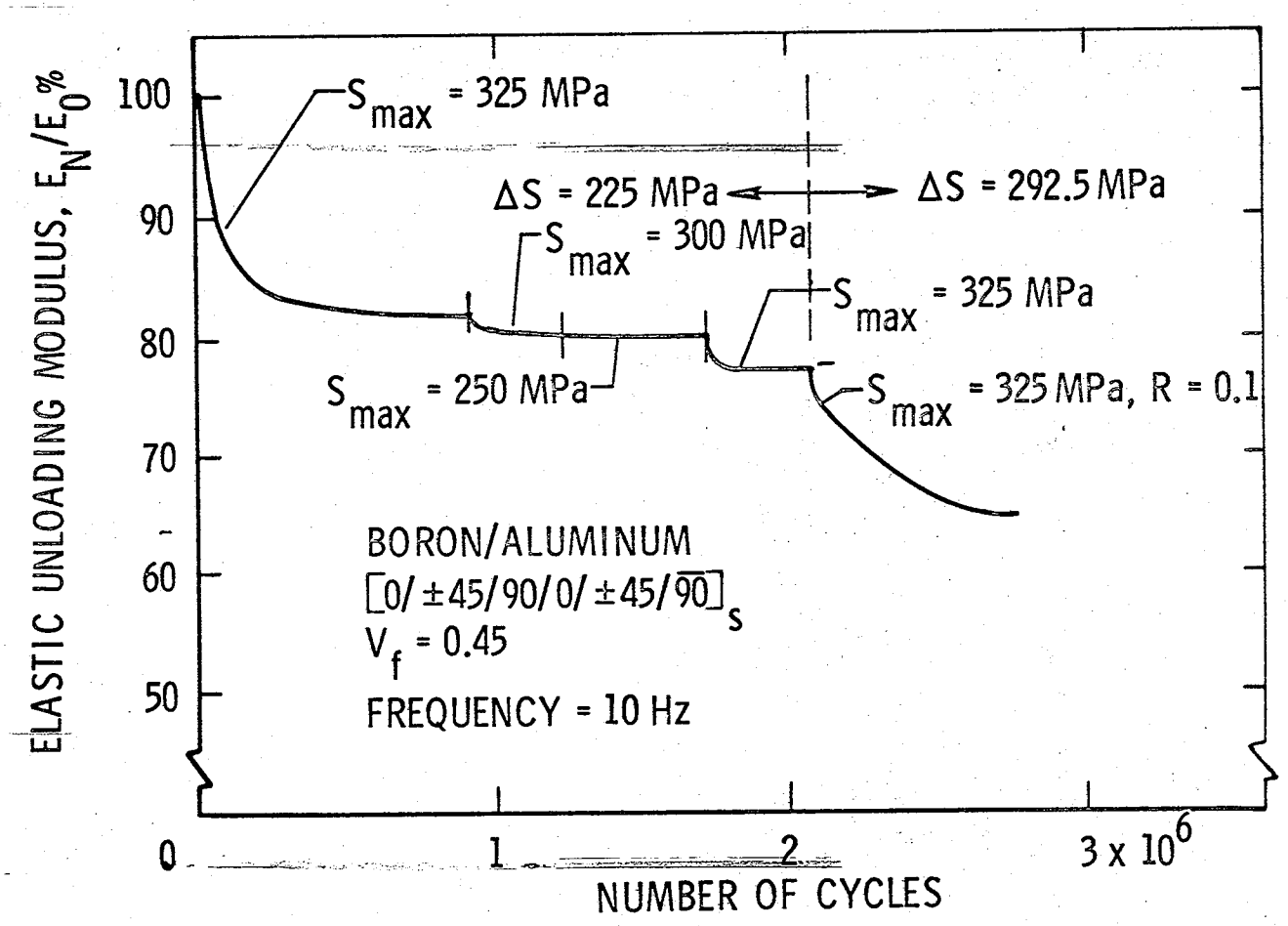

Figure 15.- Change in elastic unloading modulus under a variable loading program.

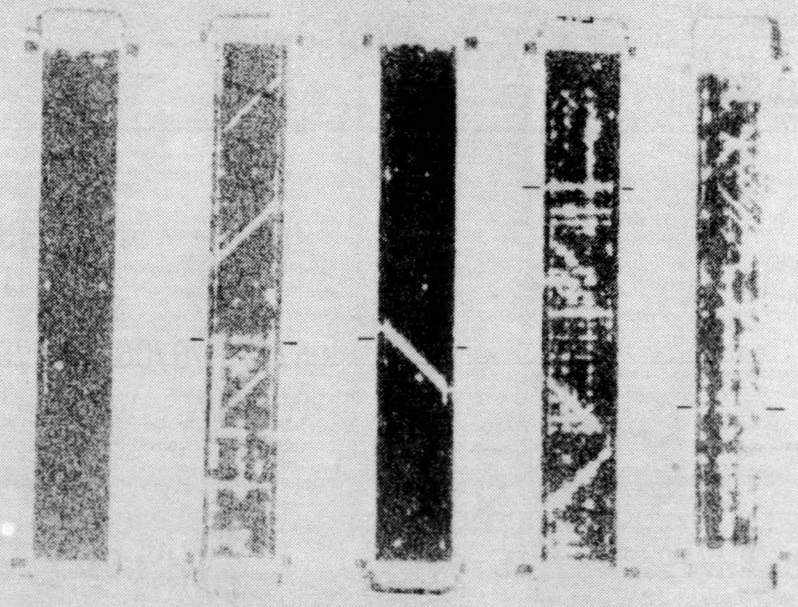

C-SCAN CLASSIFICATION	G	D	D	D	VD
MAXIMUM STRESS, MPa	375	350	375	400	338
CYCLES TO FAILURE	DID NOT FAIL AT $2x10^6$	$1.2x10^6$	$9.6x10^5$	$1.9x10^4$	$2.2x10^5$

Figure 16.- Correlation of C-scan indication, fatigue life, and fracture site.

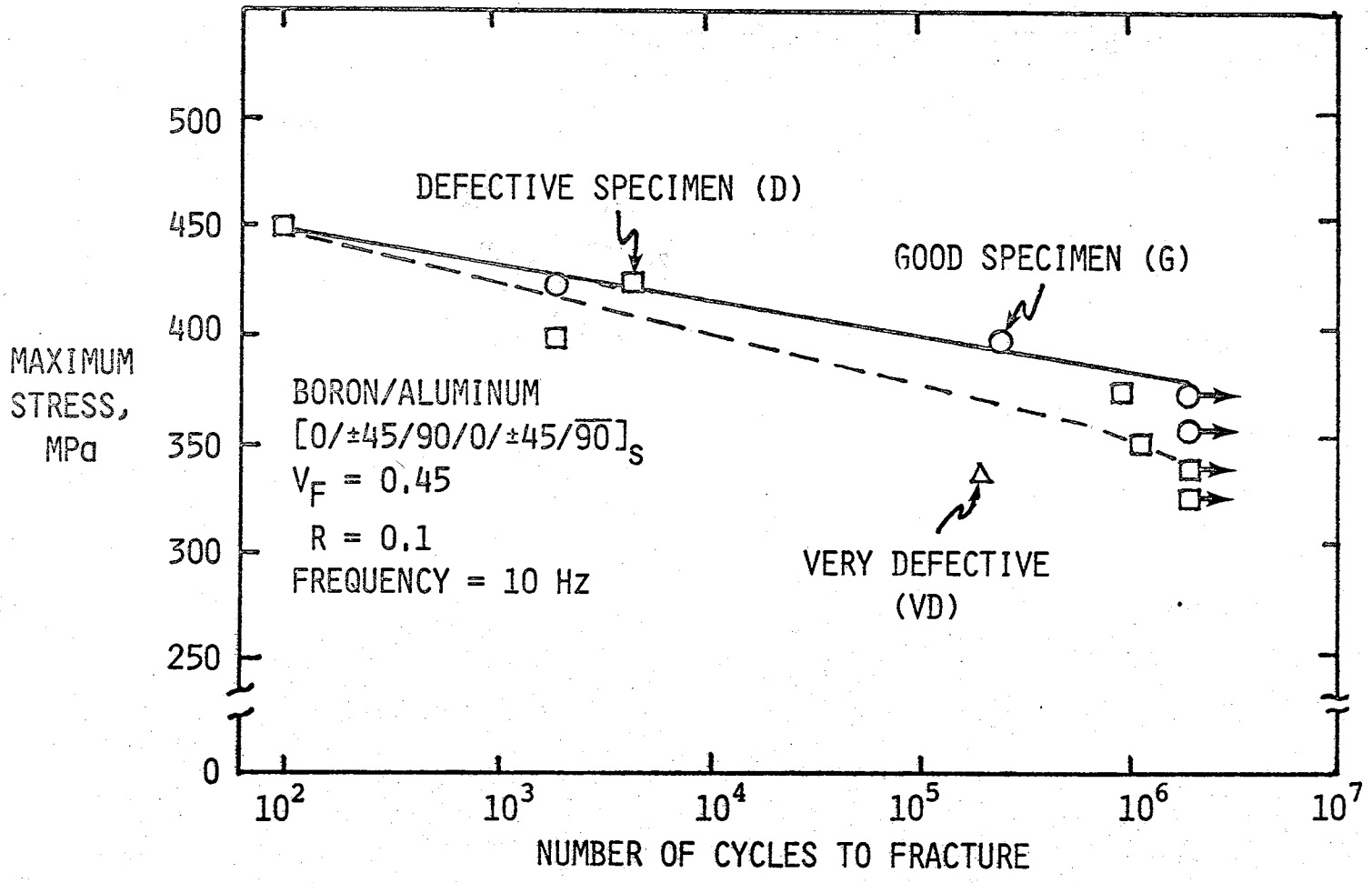

Figure 17.- Fatigue test S-N results at R = 0.1 for [0/±45/90/0/±45/90]$_S$ B/Al composite specimens.

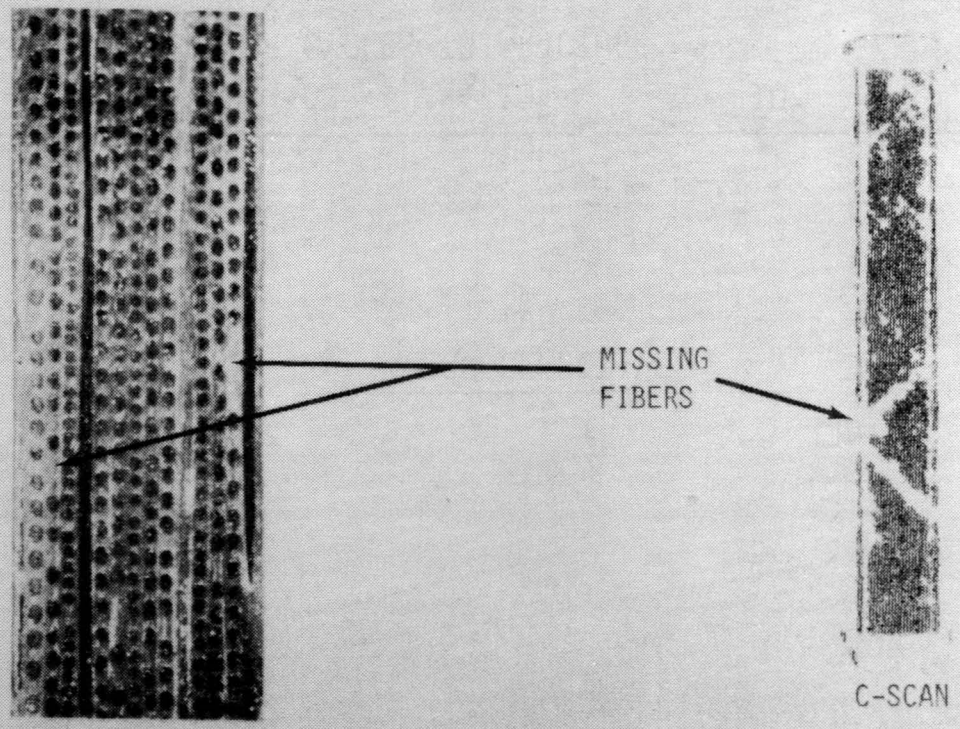

Figure 18.- Relating a C-scan indication to missing boron fibers in B/Al $[0/\pm45/90/0/\pm45/90]_S$, $V_F = 0.45$.

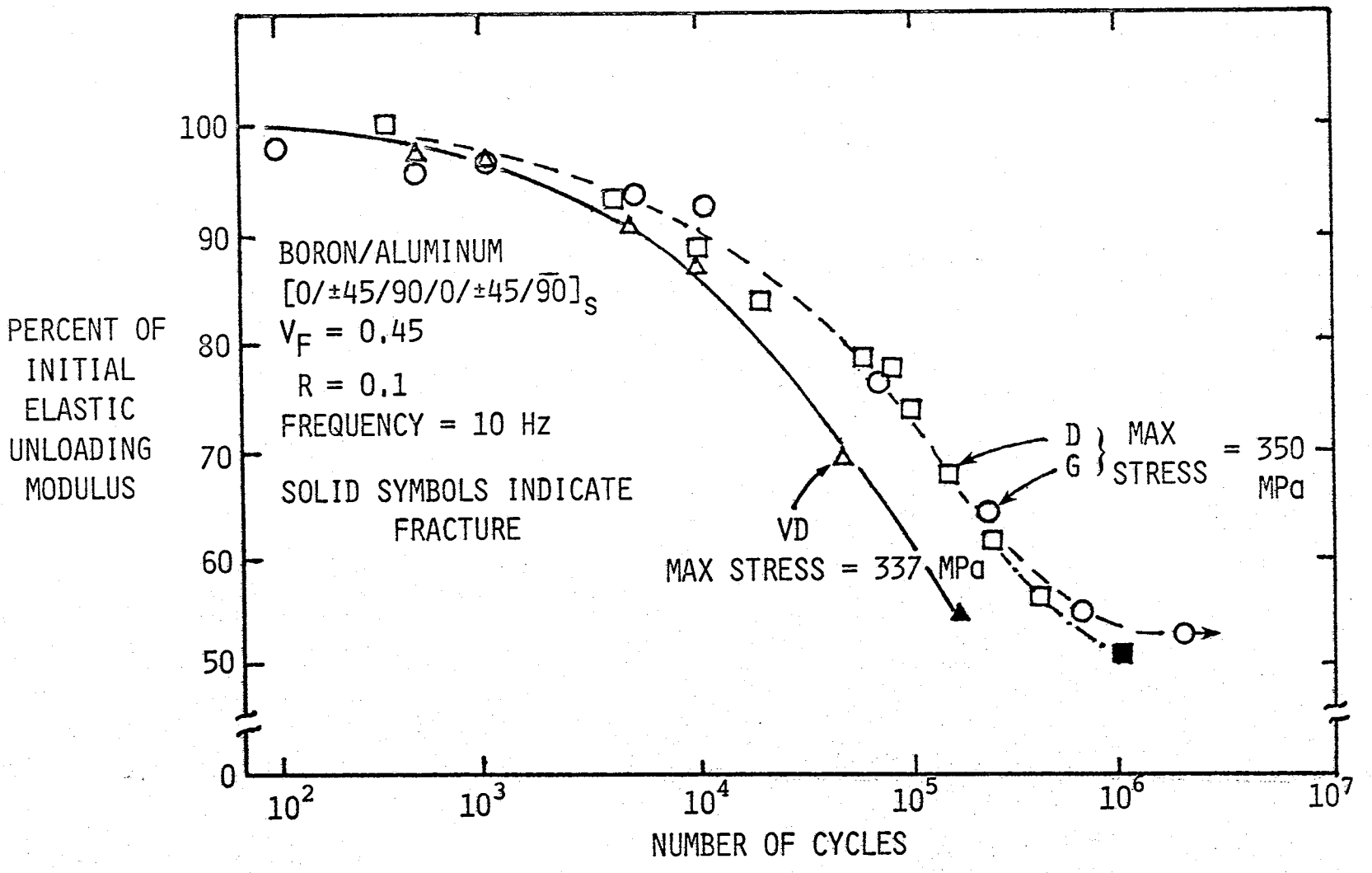

Figure 19.- Drop in elastic unloading modulus during fatigue loading.

1. Report No.	2. Government Accession No.	3. Recipient's Catalog No.
NASA TM-81926		

4. Title and Subtitle	5. Report Date
MECHANISMS OF FATIGUE DAMAGE IN BORON/ALUMINUM COMPOSITES	December 1980
	6. Performing Organization Code
7. Author(s)	8. Performing Organization Report No.
W. S. Johnson	
9. Performing Organization Name and Address	10. Work Unit No.
NASA Langley Research Center Hampton, VA 23665	506-53-23-05
	11. Contract or Grant No.
12. Sponsoring Agency Name and Address	13. Type of Report and Period Covered
National Aeronautics and Space Administration Washington, DC 20546	Technical Memorandum
	14. Sponsoring Agency Code

15. Supplementary Notes

Presented at the ASTM Symposium on Damage in Composite Materials: Basic Mechanisms, Accumulation, Tolerance, and Characterization, Bal Harbour, Florida, November 10-14, 1980.

16. Abstract

Fatigue damage mechanisms have been investigated using a series of tensile fatigue tests on several laminates of boron/aluminum (6061-0). This study focused on four aspects of the fatigue response. First, in laminates with 0° fibers on the outside, an analysis that identifies "shakedown" conditions was shown to predict the stress amplitude below which no fatigue damage accumulated. Second, a simple fatigue damage accumulation model which relates matrix fatigue cracking and the overall laminate properties is described. A model for the saturation damage stage development is presented. Third, data will illustrate that identical laminates, tested in directions 90° apart (such that one layup has 90° outer plies and the other 0°), have different fatigue behaviors due to the stacking sequence. The 90° plies on the surface develop cracks earlier than predicted by shakedown. An attempt was made to explain this stacking sequence effect. Finally, variable load history effects on the fatigue damage response were investigated by simple tests. These tests revealed that for a given stress ratio the specimen seeks the saturation damage state for the largest stress range to which it is subjected. It was also found that little damage is generated by shifting a given stress range down, whereas significant damage may be created by shifting it upward. The laminate stresses were always tensile.

17. Key Words (Suggested by Author(s))		18. Distribution Statement
Boron/aluminum composites	Fatigue	Unclassified - Unlimited
Metal matrix composites	Load history	
Fatigue damage mechanisms	Stacking sequence	
Saturation damage state		
Shakedown analysis		Subject Category 24

19. Security Classif. (of this report)	20. Security Classif. (of this page)	21. No. of Pages	22. Price*
Unclassified	Unclassified	53	A04

* For sale by the National Technical Information Service, Springfield, Virginia 22161